

Applications of Dynamic Shading Screens for Residential Buildings in Taiwan

Ben-Hsin Dow

A thesis

submitted in partial fulfillment of the
requirements for the degree of

Master of Architecture

University of Washington

2020

Committee:

Christopher Meek

Robert B. Peña

Michael Gilbride

Program Authorized to Offer Degree:

Architecture

© Copyright 2020

Ben-Hsin Dow

University of Washington

Abstract

Applications of Dynamic Shading Screens for Residential Buildings in Taiwan

Ben-Hsin Dow

Chair of the Supervisory Committee:

Christopher Meek

Department of Architecture

This thesis aims to propose a designed dynamic shading screen that is culturally and environmentally feasible for residential buildings in Taiwan. As a country located in the tropical area, Taiwan consumes a great amount of electricity on cooling. In recent years, the high cooling load in Taiwan has been causing an energy crisis and issues of air pollution during the summertime. The proposed dynamic shading screen, by saving 20% electricity consumption per household, is able to lower the cooling loads while improve daylighting quality and thermal comfort in residential buildings. Ultimately, the goal is to amplify the energy-saving per household to the country's scale in order to mitigate the issues of energy crisis and air pollution, which eventually will be beneficial to the entire living environment in Taiwan. The design of the dynamic shading screen carries on the tradition of Taiwanese window grilles. To verify the dynamic shading screen's efficacy, the device's energy-saving performance derived from energy end-use simulation will be compared with other conventional shading devices. For visualization, applications of the dynamic shading screens on an apartment and a townhouse, the two most dominant housing types, will be demonstrated. Concluding this research, a discussion of how the proposed dynamic shading screen might improve the living environment in Taiwan will be provided.

Table of Contents

Abstract

List of Figures

List of Tables

List of Charts

Chapter 1: Introduction

1.1 Climate in Taiwan

1.2 Relationship Between Climate and Electricity Consumption

1.3 Energy Generation and Consumption in Taiwan

1.4 Estimation of Annual Energy Consumption Per Household by Device

1.4.1 Annual Lighting Energy Consumption

1.4.2 Annual Equipment Energy Consumption

1.4.3 Annual Cooling Energy Consumption

1.4.4 Annual Energy Consumption per Household.

1.5 Current Conditions of Residential Buildings in Taiwan

Chapter 2: Taiwanese Window Grilles

2.1 Tradition of Taiwanese Window Grilles

2.2 Current Uses of Window Grilles

Chapter 3: Precedents Study of Dynamic Shading Devices

3.1 Simple Shading Models

3.1.1 Louvers and Fins

3.1.2 Foldable Panels

3.1.3 Electrochromic Glazing (EC Glazing)

3.2 Complex Shading Models

3.2.1 Origami (Kaleidocycle Façade)

3.2.2 Biomimetic Structure

3.2.3 Hexagonal Façade Skin

3.2.4 Shape Variable Mashrabiya (SVM)

Chapter 4: Methodology

4.1 The Prototype of the Dynamic Shading Screen

4.2 Settings in the Computational Simulation

4.2.1 Housing Typologies

4.2.2 Solar Radiation Intensity Testing

4.2.3 Energy Model of An Apartment

4.2.4 Energy Model of a Three-story Townhouse

4.3 Calibration of the Energy Models

4.4 Variables in the Simulation

Chapter 5: Results

- 5.1 Results from the Townhouse Model
- 5.2 Results of from the Apartment Model

Chapter 6: Visualization

- 6.1 Visualization of an Apartment
- 6.2 Visualization of a Townhouse
- 6.3 Visualization of a Townhouse Interior

Chapter 7: Luminance and Illuminance Testing

- 7.1 False-Color Luminance Distribution
- 7.2 Point-in-Time Illuminance Range
- 7.3 Annual Illuminance Testing

Chapter 8: Conclusion

- 8.1 Benefits for Residence's Occupants
- 8.2 Benefits for Taiwan

Bibliography

List of Figures

- Figure 1:** Average high/low temperature by month in Taipei city from 2015 to 2019.
- Figure 2:** Sun shading charts of Taiwan derived from Climate Consultant 6.
- Figure 3:** Monthly mean temperature in Taipei city in 2018.
- Figure 4:** Monthly electricity consumption in Taiwan in 2018.
- Figure 5:** Power generation in Taiwan by fuel
- Figure 6:** The air quality of Taipei city in 2018.
- Figure 7:** Electricity consumption by sector.
- Figure 8:** Annual electricity consumption per household.
- Figure 9:** The lack of shading strategies on the modern residential buildings
- Figure 10:** Window grilles on residential buildings.
- Figure 11:** Multifarious patterns of traditional window grilles prevailed in 1970s.
- Figure 12:** Anti-theft version of a window grille.
- Figure 13:** Opening extension version of a window grille.
- Figure 14:** A utility space enclosed by a window grille.
- Figure 15:** The varying rotation angles of the louver's and fin's slats.
- Figure 16:** Simplified prototype of parametric camshaft
- Figure 17:** Different states of the foldable panels.
- Figure 18:** Range of tint of an electrochromic window.
- Figure 19:** Kaleidocycle rotation motions.
- Figure 20:** The proposed biomimetic geometry in Jahanara's research.
- Figure 21:** Two operational modes of the hexagonal pattern.
- Figure 22:** Shape Variable Mashrabiya (SVM).
- Figure 23:** The prototype of dynamic shading screen adapted from the window grilles.
- Figure 24:** The percentage of different housing types in Taiwan.
- Figure 25:** Climate zone in the U.S. defined by ASHRAE.
- Figure 26:** Pie charts for energy model verification.
- Figure 27:** Orientations assigned to the townhouse's and the apartment's energy models.
- Figure 28:** A tree diagram of variables in the energy end-use simulation.
- Figure 29:** A façade design that could be used to integrate the dynamic shading screen with a mid-rise apartment.
- Figure 30:** Orientation of the designed apartment.
- Figure 31:** Apartment with dynamic shading screens at 7 am.
- Figure 32:** Apartment with dynamic shading screens at 10 am.
- Figure 33:** Apartment with dynamic shading screens at 12 pm.

Figure 34: Apartment with dynamic shading screens at 1 pm.

Figure 35: Apartment with dynamic shading screens at 3 pm.

Figure 36: Apartment with dynamic shading screens at 5 pm.

Figure 37: A set of dynamic shading screen that can be installed on an existing residential building.

Figure 38: Options of the frames and fins.

Figure 39: The application of dynamic shading screen on an existing townhouse.

Figure 40: Orientation of the townhouse.

Figure 41: The townhouse with dynamic shading screens at 10 am.

Figure 42: The townhouse with dynamic shading screens at 12 pm.

Figure 43: The townhouse with dynamic shading screens at 1 pm.

Figure 44: The townhouse with dynamic shading screens at 3 pm.

Figure 45: The townhouse with dynamic shading screens at 4 pm.

Figure 46: The interior of a townhouse with dynamic shading screens at 9 am.

Figure 47: The interior of a townhouse with dynamic shading screens at 12 pm.

Figure 48: The interior of a townhouse with dynamic shading screens at 1 pm.

Figure 49: The interior of a townhouse with dynamic shading screens at 2 pm.

Figure 50: The interior of a townhouse with dynamic shading screens at 3 pm.

Figure 51: The interior of a townhouse with dynamic shading screens at 4 pm.

Figure 52: The interior of a townhouse with dynamic shading screens at 5 pm.

Figure 53: The interior of a townhouse with dynamic shading screens at 8 pm.

Figure 54: The interior of a townhouse with dynamic shading screens at 10 pm.

Figure 55: The study townhouse for luminance and illuminance testing.

Figure 56: A section cut of the townhouse.

Figure 57: False-color luminance scale

Figure 58: False-color luminance distribution A.

Figure 59: False-color luminance distribution B.

Figure 60: False-color luminance distribution C.

Figure 61: False-color lux scale from 0 to 3000 lux.

Figure 62: Point-in-time illuminance range A.

Figure 63: Point-in-time illuminance range B.

Figure 64: Point-in-time illuminance range C.

Figure 65: Annual illuminance received in the townhouse's study area in percentage of hours in a year.

Figure 66: Annual illuminance within 100 to 3,000 lux in percentage of hours.

Figure 67: Annual illuminance above 3,000 lux in percentage of hours.

List of Table

- Table 1:** The annual electricity consumption by lighting per household.
- Table 2:** The annual electricity consumption by equipment per household.
- Table 3:** Applicability of air conditioner by square footage published by *Foundation of Taiwan Industry Service*.
- Table 4:** The annual cooling consumption by equipment per household.
- Table 5:** IES illuminance level standard for different types of industries.
- Table 6:** Control strategies of the tint of EC glazing.
- Table 7:** Mean solar radiation gained in each orientation.
- Table 8:** The settings in the apartment energy model.
- Table 9:** The settings in the townhouse energy model.
- Table 10:** Summary of power plants in Taiwan

List of Chart

- Chart 1:** Electricity Consumption in Townhouse (Orientation: north south).
- Chart 2:** Electricity Consumption in Townhouse (Orientation: east west).
- Chart 3:** Electricity Consumption in Apartment (Orientation: south west).
- Chart 4:** Electricity Consumption in Apartment (Orientation: south east).
- Chart 5:** Summary of electricity consumption in the townhouse.
- Chart 6:** Summary of electricity consumption in the apartment.

Acknowledgements

I would like to express my deep and sincere gratitude to Prof. Christopher Meek, Chair of my committee; Prof. Rob Peña; and Michael Gilbride for their continued support and encouragement. In addition, I would like to thank all the resources and technical supports from Integrated Design Lab (IDL) in the Department of Architecture, University of Washington. My completion of this thesis could not have been accomplished without all of these prerequisites.

I am deeply indebted to my parents, especially my father Dr. Wei-Ping Dow who had been supporting me in all aspects. Without you, I would never have the opportunity to study abroad and gain all the invaluable experiences. My heartfelt thanks.

1.1 Climate in Taiwan

Located at the boundary between subtropical and tropical region, with 22 to 25 degrees north latitude and surrounded by ocean, Taiwan is subjected to hot and humid climate. The line chart of average high/low temperature [1] shows that throughout a year the temperature in Taiwan is generally high. Especially during the summertime, the average high temperature is usually close to a hundred-degree Fahrenheit (Figure 1). The sun shading diagram also shows that solar shading is highly beneficial to most of the year. There is only a short amount of time when the country is cool without shading (Figure 2).

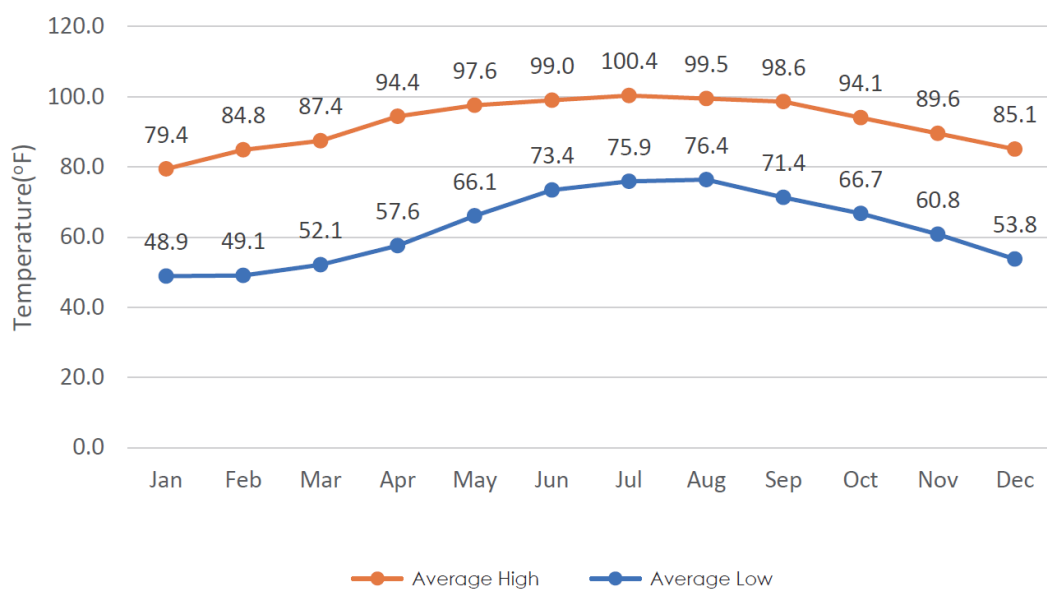


Figure 1. Average high/low temperature by month in Taipei city from 2015 to 2019.

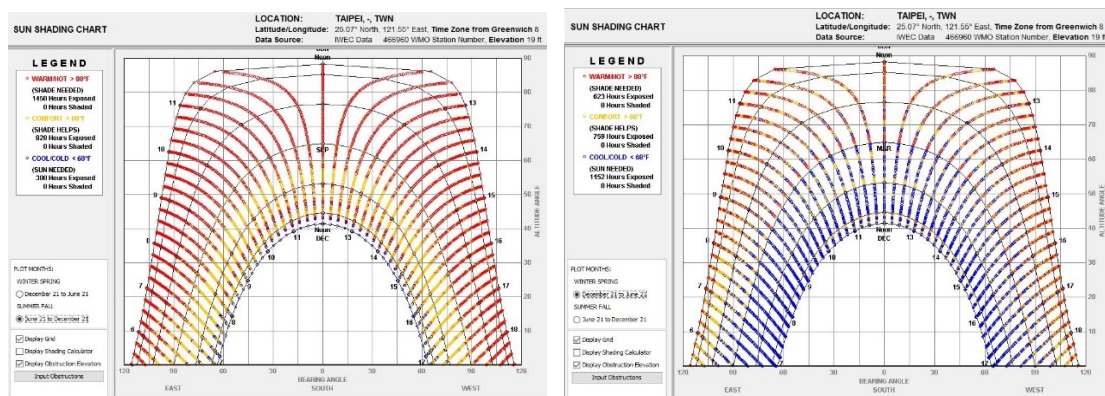


Figure 2. Sun shading charts of Taiwan derived from the UCLA-produced Climate Consultant 6 climate analysis tool [2] show the need for of shading throughout a year. The chart on the left shows the time period from June to December. The chart

on the right shows the time period from December to June.

1.2 Relationship Between Climate and Electricity Consumption

To verify the relationship between the electricity consumption and the climate, statistical data are collected from Taiwanese Bureau of Energy [3] and Central Weather Bureau [4]. A comparison between Figure 3, 4 shows the positive correlation between monthly electricity consumption and mean temperature. It is clear to see that the monthly electricity consumption is peaking along with the monthly mean temperature especially from June to August. The period is the time when the Taiwanese government usually advocates for economizing energy use to the public. Based on this trend, an assumption is made: the cooling load in residential buildings is one of the driving factors behind the fluctuation in the national electricity consumption. The assumption will be verified and discussed in the following paragraph.

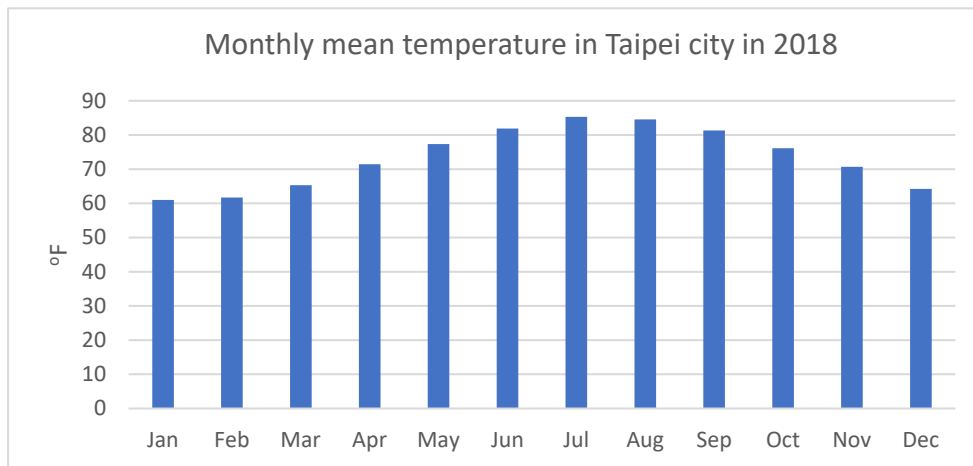


Figure 3. Monthly mean temperature in Taipei city in 2018.

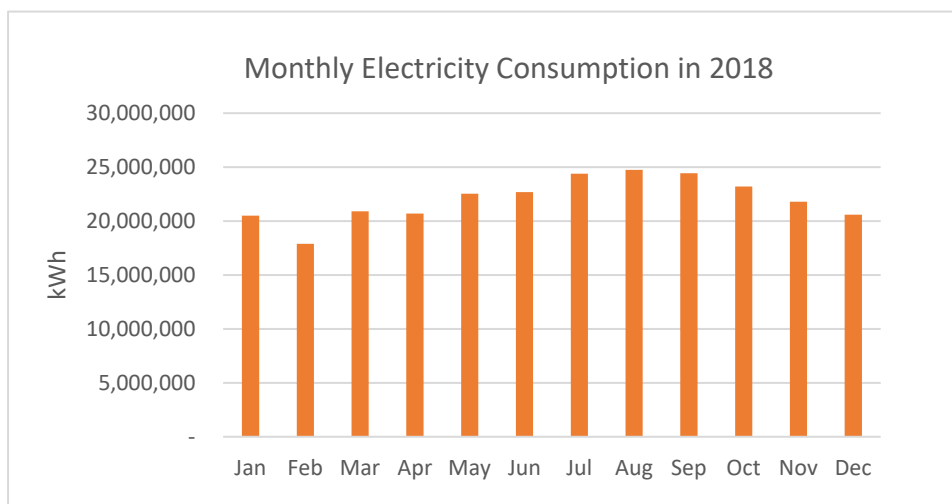


Figure 4. Monthly electricity consumption in Taiwan in 2018.

1.3 Energy Generation and Consumption in Taiwan

To identify the latency behind the energy generation that contaminates the air quality, the data of energy generation by fuels are collected (Figure 5). Fossil fuels, including coal, oil, and natural gas are the dominant power sources in Taiwan, which account for approximately 80% of the national power generation since 2007. Nuclear power is the secondary fuel following the fossil fuels. Renewable energy still accounts for only 3% to 5% until 2017 in spite of the government’s sustained promotion of its use.

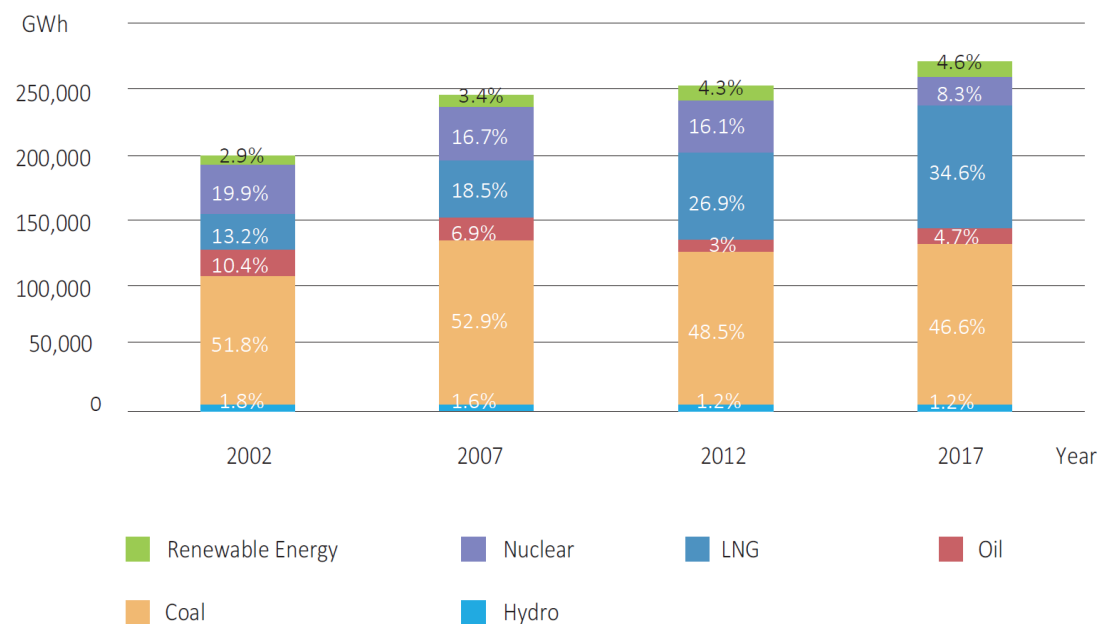


Figure 5. Power generation in Taiwan by fuel published by *Taiwanese Bureau of Energy* [5].

However, due to warming weather associated with climate change, the demands of cooling increase yearly. In recent years, Taiwan has confronted an energy crisis during the summertime. Each power plant has to reach its maximum capacity to meet the demanded peak loads. In 2016 when Jinshan Nuclear Power Plant, the first nuclear power plant built in Taiwan, was decommissioned due to its age and condition, the electrical loads were transferred to other sources, primarily thermal power plants. The heavy reliance on thermal power plants produces substantial CO₂ emissions and suspended particles, which is one of the reasons behind the air pollution among several cities (Figure 6).



Figure 6. The air quality of Taipei city in 2018.

To understand the amount of electricity that is consumed by residential buildings, electricity consumption data by sector published by Taiwanese Bureau of Energy were collected (Figure 7). The bar chart shows that industry consumes about 50% of the total energy, which coincides with the fact that there are many semiconductor manufacturing and traditional factories in Taiwan. Residential and commercial sectors are the secondary contributors. Each of them consumes 18% to 20% of the total energy consumption.

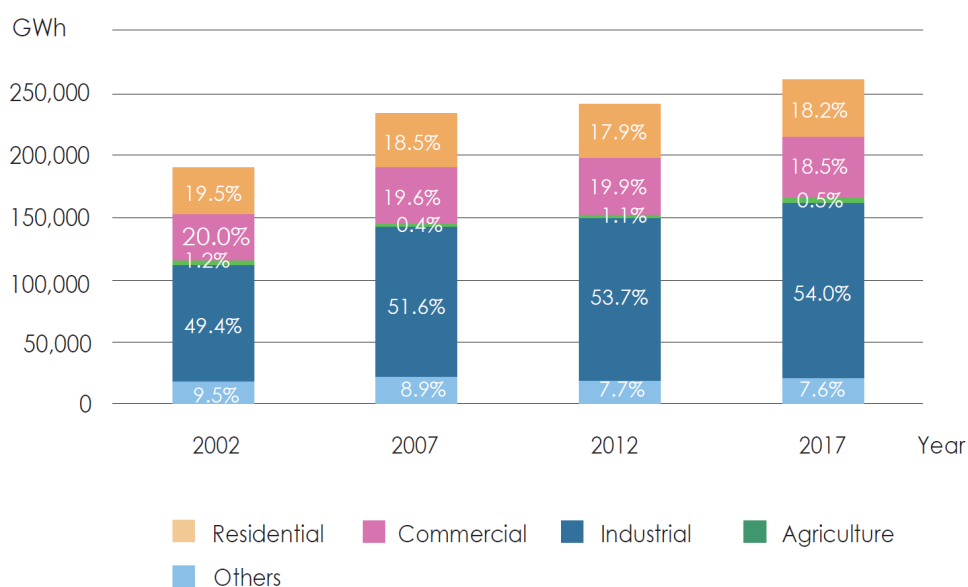


Figure 7. Electricity consumption by sector [5].

To verify the assumption made in the previous paragraph that the cooling load in residential buildings is one of the driving factors behind the fluctuation of electricity consumption, an estimation of annual energy consumption per household by device has been completed. Considering the number of occupants and the occupants' behavior will impact the energy consumption, a four-person-family's behavior is set for establishing the testing scenario. The scenario of the household is described as follows:

1. There are four members living in the household: two parents and two children.
2. The parents go to work, and the children go to school from 9 am to 6 pm during weekday, and they stay at home during weekend.
3. The parents live in a master bedroom and each child has their own bedroom.
4. Each bedroom has one air conditioner which is used only six months in a year, April to September.
5. The family cook dinner every day at home so that equipment in kitchen is used every day.

1.4 Estimation of Annual Electricity Consumption Per Household by Device

The estimation of electricity consumption by device includes the use of cooling systems, lighting, and the most used equipment. The estimation will be used as a metric for calibrating the parameters in the future energy end-use simulation. Part of the wattage data of the equipment have been collected from *Technical Manual for Energy-saving in Residences* published by Bureau of Energy [6]. The rest of the data were calculated based on the equipment's wattage published by manufacturers and an estimated use time. The cooling and lighting energy consumption are estimated based on the product's specifications published by manufacturers and an estimated use time (hours/year) and an estimated schedule.

1.4.1 Annual Lighting Energy Consumption

Six 11W LED bulbs are assigned to each room except the living room (Table 1). In the living room, eight linear LED lights are set to reflect the typical lighting configuration. The use time of 2880 hours a year is calculated based on the 8-hour use time in a day. Accordingly, the total annual lighting energy consumption per household is 1157.8 kWh.

Room Type	Lighting Device	Number of Device	Use Time/Year (Hours)	Energy Consumption/Room Year (kWh)
Living Room	Linear LED light (9w) *1	8	(8 hr) x (30 D) x (12 M) = 2880	207.3
Dining Room	LED Bulb (11W)	6	2880	190.1
Kitchen	LED Bulb (11W)	6	2880	190.1
Master Bedroom	LED Bulb (11W)	6	2880	190.1
Bedroom x2	LED Bulb (11W)	6x2	2880	380.2
Total Annual Lighting Energy Consumption per Household				1157.8

Table 1. The annual electricity consumption by lighting per household.

*1: The wattage data is collected from the product specification on PHILIPS website [7].

1.4.2 Annual Equipment Energy Consumption

The wattage and the use time of the most used equipment is given by the *Technical Manual for Energy-saving in Residences* published by Bureau of Energy [6] except for the data of refrigerator and dishwasher, noted in Table 2. The total annual equipment energy consumption per household is 3416 kWh.

Other Equipment	Wattage of Device (W)	Number of Device	Use Time/Year (Hours)	Energy Consumption/Device Year (kWh)
Refrigerator	200 *2	1	(4 hr) x (30 D) x (12 M) = 1440	288
Domestic water heater	8800	1	(2/3 hr) x (30 D) x (12 M) = 240	2112
Microwave oven	1200	1	(1/10 hr) x (30 D) x (12 M) = 36	43.2
Washing machine	500	1	(1/2 hr) x (8 D) x (12 M) = 48	24
Dishwasher	375 *3	1	(2 hr) x (30 D) x (12M) = 720	270
Thermos	800	1	(2 hr) x (30 D) x (12 M) = 576	460.8
Rice cooker	800	1	(1/3 hr) x (22 D) x (12 M) = 88	70.4
TV	120	1	(3 hr) x (30 D) x (12 M) = 1080	129.6
Computer	200	2	(2 hr) x (30 D) x (12 M) x 2 = 1440	288
Total Annual Equipment Energy Consumption per Household				3686

Table 2. The annual electricity consumption by equipment per household.

*2: The energy consumption of the refrigerator is collected from Panasonic [8].

*3: The energy consumption of the dishwasher is collected from Bosch [9].

1.4.3 Annual Cooling Energy Consumption

Lastly, the cooling energy consumption is estimated in this research. One air conditioner is assigned to each room described in Table 1 according to its square footage referencing Table 3. For the living room and the dining room, which are usually layout as a large space without partitions, an AC with larger capacity is assigned. Due to its high wattage, the use time is divided into weekday and weekend schedules to reflect the occupant’s different patterns of use. On weekdays, it assumes that the AC is turned on three hours from 6 pm to 9 pm during dinner time. On weekends, as the occupants may spend more time in the living room and the dining room, five hours are scheduled.

For the bedrooms, 8 hours are scheduled to reflect the usage during bedtime. All AC units are only used for 6 months of the year, from April to September, when the temperature is usually higher than the remaining months. In addition to AC units, fans are assigned to each room. It assumes that each fan is used eight hours a day from March to October. The total annual cooling energy consumption per household is 9876 kWh (Table 4).

AC Capacity				Applicable Square Footage	
Kcal/hr	BTU/hr	KW	Refrigeration Ton (RT)*5	Ft ²	Pyeong *4
2,000	8,000	2.32	0.8	110	3
2,500	10,000	2.90	1	110 - 180	3-5
3,150	12,600	3.66	1.26	140 - 210	4-6
3,550	14,200	4.12	1.42	180 - 250	5-7
5,600	18,000	5.23	1.8	210 - 280	6-8
6,300	22,400	6.51	2.24	280 - 350	8-10
7,500	25,200	7.32	2.52	350 - 430	10-12
8,000	30,000	8.72	3.0	430 - 530	12-15
9,000	32,000	9.30	3.2	430 - 640	12-18
10,000	36,000	10.46	3.6	530 - 640	15-18

Table 3. Table of air conditioner applicability by square footage published by *Foundation of Taiwan Industry Service* [10].

*4: 1 pyeong = 35.58 ft² [11].

*5: Refrigeration Ton (RT), also called ton of refrigeration, is a unit of power used in some countries to describe the heat-extraction capacity of refrigeration and air conditioning equipment. 1 RT = 10 kBUT/hr [12].

Room Type	Wattage of Device	Number of Device	Use Time/Year (Hours)	Energy Consumption/Room Year (kWh)
Living + Dining Room (Weekday)	8720W	1	(3 hr) x (22 D) x (6 M) x 0.5 = 198	1726.56
Living + Dining Room (Weekend)	8720W	1	(5 hr) x (8 D) x (6 M) x 0.5 = 120	1046.4
Mater Bedroom	3600W	1	(8 hr) x (30 D) x (6 M) x 0.5 = 720	2592
Bedroom x2	2800W	2	(8 hr) x (30 D) x (6 M) x 0.5 = 720	4032
Fans	50	5	(8 hr) x (30 D) x (8 M) x 5 = 9600	480
Total Annual Cooling Energy Consumption per Household				9876.96

Table 4. The annual cooling consumption by equipment per household.

1.4.4 Annual Electricity Consumption per Household.

In summary, the annual energy consumption of cooling, lighting, and equipment is 9876, 1157, and 3686 kWh respectively (Figure 8). Cooling accounts for two-third (67%) of the total electricity consumption per household. The result will also be used for calibrating the parameters in the energy end-use simulation in the following chapter.

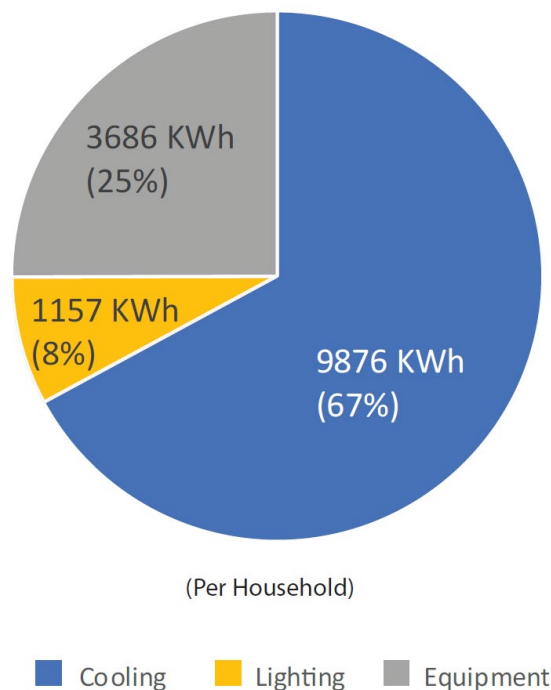


Figure 8. Annual electricity consumption per household.

1.5 Current Conditions of Residential Buildings in Taiwan

The inclusion of shading elements in building design has historically been one of the most used strategies to help mitigate the threats of space overheating and discomfort in hot regions. Given the fact that residential buildings in Taiwan consume a significant proportion of electricity on cooling, are shading devices commonly used on residential buildings in the country? Surprisingly, not. Most of the residential buildings built in and before the early 21st century do not have effective shading strategies in response to the climate. The prevailing design language of simplicity and consistency highlights the aesthetic consideration and eliminates the performative function (Figure 9). Interestingly, instead of having shading devices, there is a commonly used façade attachments on townhouses and mid-rise apartment which is window grilles. Window grilles can be seen on many buildings constructed in the late 20th century (Figure 10).



Figure 9. The lack of shading strategies on modern residential buildings.

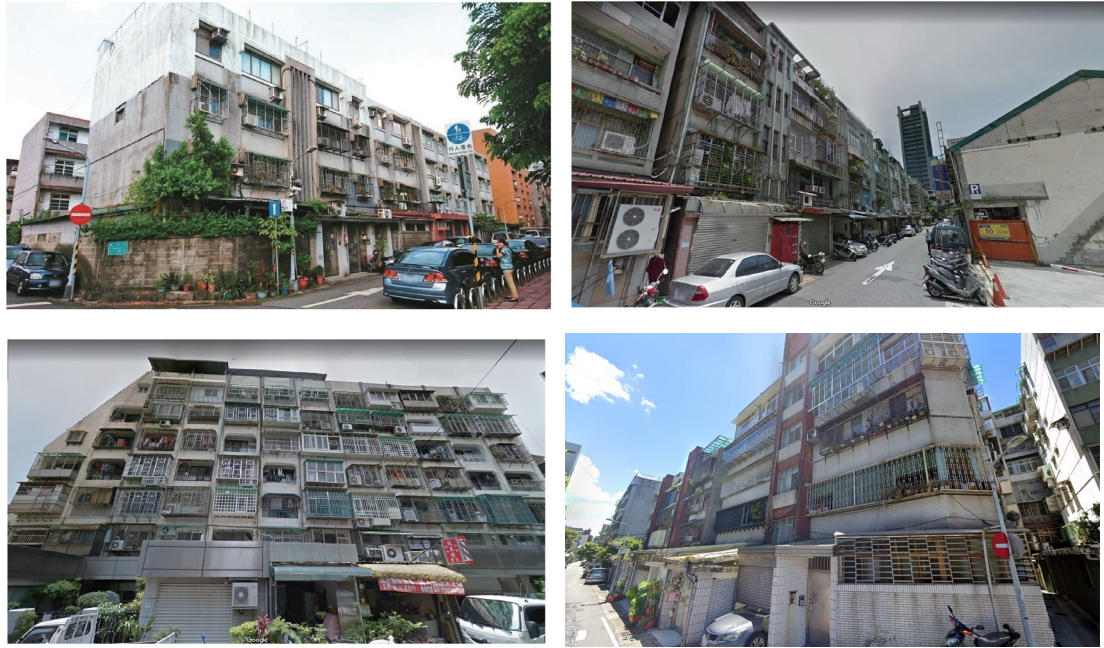


Figure 10. Window grilles on residential buildings.

Chapter 2: Taiwanese Window Grilles

2.1 Tradition of Taiwanese Window Grilles

Originally, window grilles emerged in Taiwan in the 1920s. As a vernacular decoration, window grilles were mainly used for the windows of temples and houses. As Taiwan's economy grew in 1970s, Taiwanese people had had the financial ability to buy houses. However, public security was not improved in pace with the economy. Due to crime and particularly frequent break-ins, window grilles became prevalent to prevent theft. Other than this practical function, a growing attention to aesthetics of houses is another reason behind the prevalence. Furthermore, local craftsmen sought to compete with one another, creating unique and expressive designs that reflected pride in their fabrication skills [13].

Patterns of the window grilles had no restrictions beyond the functions of security and basic structural integrity (Figure 11). They were mainly designed and fabricated by local craftsmen, and some were customized according to the houseowner's requests. The most common pattern was the combination of lines and arcs. During its most prominent period, more lively geometry, such as pattern of flora, mountain, and musical note could also be seen.



Figure 11. The multifarious patterns of traditional widow grilles prevailed in 1970s [13].

However, such craftsmanship disappeared in the late 1990s due to the emergence of new materials and architectural typology, and because of maintenance concerns such as deterioration and rusting. Thus, the traditional window grilles were eventually replaced by stainless steel window grilles which are easier to be manufactured in factories but lack vitality and aesthetic diversity.

2.2 Current Uses of Window Grilles

In the present day, despite that the social and economic context have changed and crime and theft are uncommon in the society, in Taiwanese culture, people still tend to install window grilles as a means to provide a sense of safety. Some window grilles have even been modified to suit different uses and architectural typologies. Three current uses of window grilles that can be commonly seen on residential buildings are categorized below.

The basic version of the window grille, which is usually installed on a punched window condition, provides the single function of anti-theft (Figure 12). An adaptation of this version with a depth extending beyond a punched window and with a piece of canopy attached above is usually used to extended openings (Figure 13). People usually put their potted plants within the little space created by the window grilles. The last version is an enclosure that is usually attached to the parapet of an outdoor terrace, which is commonly used as a utility space or an outdoor laundry room (Figure 14). People tend to put the washing machine and hang their clothes to dry there.



Figure 12. Anti-theft version of a window grille.

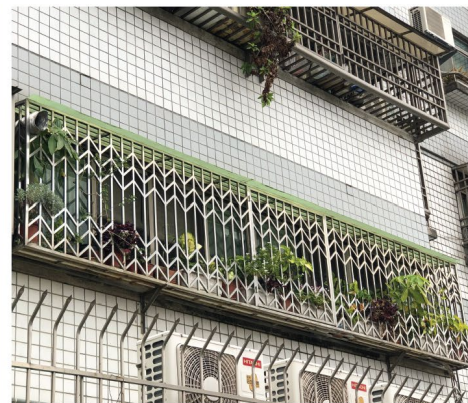


Figure 13. Opening extension version of a window grille.



Figure 14. A utility space enclosed by a window grille.

Chapter 3: Precedents Study of Dynamic Shading Devices

Current studies on dynamic shading devices are categorized into two types in this research: simple shading models versus complex shading models, depending on the configuration and operation of the devices. For this research louvers, foldable panels, and electrochromic glazing are included in the simple shading models, while dynamic skin, geometry-based grid, and shape variable screens are categorized into the complex shading category.

3.1 Simple Shading Models

3.1.1 Louvers and Fins

A study in Abu Dhabi [14] was conducted to explore the influence of external dynamic louvers on the energy consumption of an office building. The testing scenario was set up in computational program by building modules of the office building. The main variation of the simulation was the slat angles of the external louvers varying from -80 to +80 degrees in 20 degrees increments (Figure 15). In order to respond to the sun position, the louvers on the southern façade were arranged horizontally, while on the eastern and western façade the louvers were set up vertically. The proposed control strategy of the louvers' slat angle aimed to minimize the total lighting and HVAC energy consumption at the given time. The results were that when coupled with light dimming system, the dynamic louvers achieved energy savings by 34.02%, 28.57% and 30.31% on the southern, eastern, and western facades respectively compared to no shading.

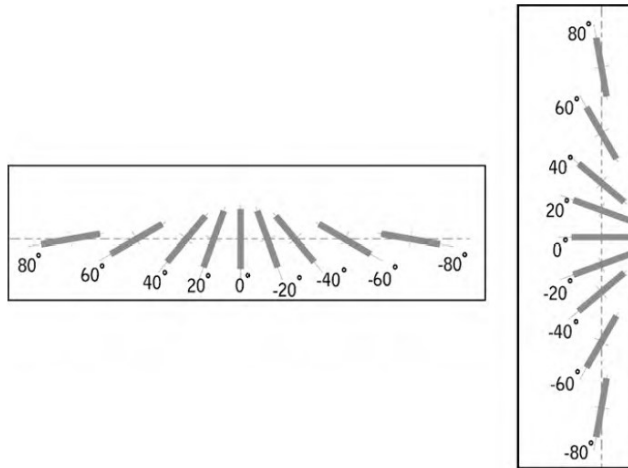


Figure 15. The varying rotation angles of the louver's and fin's slats [14].

A concern proposed by the study is that the energy-saving performance of the static shading device, if the slats are titled appropriately, is close to the performance of dynamic shading devices. Considering the cost of installation and the durability of the dynamic shading device, the financial worthiness needs to be evaluated.

A study in Greece [15] was conducted to examine a dynamic control strategy for an exterior non-retractable louver system in offices. The study evaluated the settings of different external louver's slat angles from 0 to 90 degrees with 10 degrees increments. Different from the study mentioned above, this study further evaluated different configuration between louvers' slat angles and window to wall ratio (WWR). The result shows that both static and dynamic shading device reduce the load of cooling, and the effect is more significant for scenario that has higher window to wall ratio. In WWR 80%, WWR 60%, and 40% scenarios, dynamic shading device reduce 27%, 16%, and 6% cooling load respectively compared to a static shading device. However, in all scenarios, either static shading device or dynamic shading device increase the loads of heating and lighting.

Another study in Indonesia [16] was conducted to design a parametric camshaft mechanism to control the slat angle of louvers. The studying building was a Small Office Home Office (SOHO) in which different types of industries could be the potential tenants. This study used Illuminating Engineering Society (IES) indoor lighting standards in which illuminances from 350 to 750 lux were ranged to meet the needs of different industries (Table 5). The author concluded that the louvers' slat angle from 15 to 75 degrees will make the indoor lighting condition fall into the range of 350 to 750 lux illuminance. Accordingly, a strategy of designing a set of

parametric camshafts to control the louvers slat angles was created (Figure 16).

This study optimized louvers' slat angle at specific time assuming the louvers would be motored accordingly. It established an operational strategy that optimized the louvers' slat angles for given time period.

	Types of creative industries	IES Standard
I	Architecture	750 lux
	Design	
	Fashion	
II	Handycraft Store	600 lux
	Craft	
III	Advertising	500 lux
	Video, Film, Photography	
	Interactive Games	
	Publisher	
	Research & Development	
	Computer Services	
IV	Performing Art	350 lux
	Music	
	Radio	
	Television	

Table 5. IES illuminance level standard for different types of industries [16].

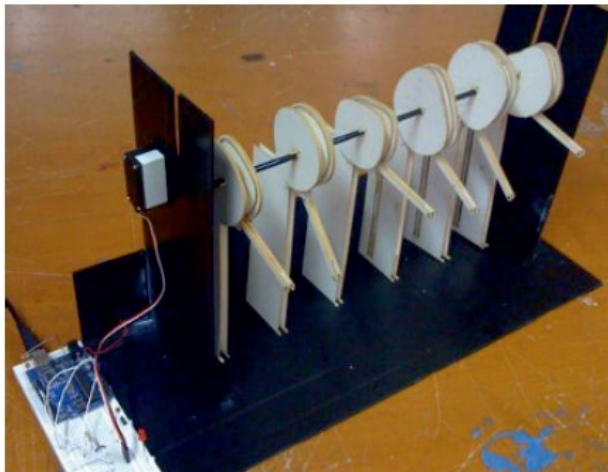


Figure 16. Simplified prototype of parametric camshaft [16].

The result shows that the proposed control strategy successfully makes the illuminance level fall into the required ranges for each types of industries. However, the author concluded that the proposed parametric camshaft mechanism was designed specifically for area site location that has two-seasonal climate conditions.

For other areas that have different climate conditions, the efficiency and benefits of the system would be impaired, unless modified accordingly.

3.1.2 Foldable Panels

Mostafa M. S. Ahmed et al. conducted an experiment of using a set of foldable panels as a shading device in Egypt [17]. The device was assembled with two aluminum panels and foldable frames (Figure 17). Indoor and outdoor weather conditions were collected by sensors, processed by software Grasshopper (a visual programming language and environment that runs within the Rhinoceros [18]) in Rhinoceros (a commercial 3D computer graphics and computer-aided design (CAD) application software developed by Robert McNeel & Associates [19]), and used as data to control the device. When closed-mode is needed, the device will be automatically extended to cover the whole window, while when open-mode is needed, the device can be automatically folded as a single-layer or two-layer horizontal shading device. The result of the experiment shows the comparison of the indoor temperature with and without the kinetic shading device during July to August. When the outdoor temperature is higher than 28°C (82.4°F) (the upper comfort limitation, defined by the Adaptive Comfort Standard metric), the indoor temperature without the shading device will exceed 28°C (82.4°F), whereas with the shading device the indoor temperature is effectively controlled under 28°C (82.4°F).

In terms of energy savings, the study shows the comparison of average monthly electricity consumption before and after the installation of the shading device. Before the installation, the building consumed approximately 450 kWh (total electricity consumption) per month. After installing the shading system, the building consumed 330 kWh, which is 26% saving compared to the baseline.

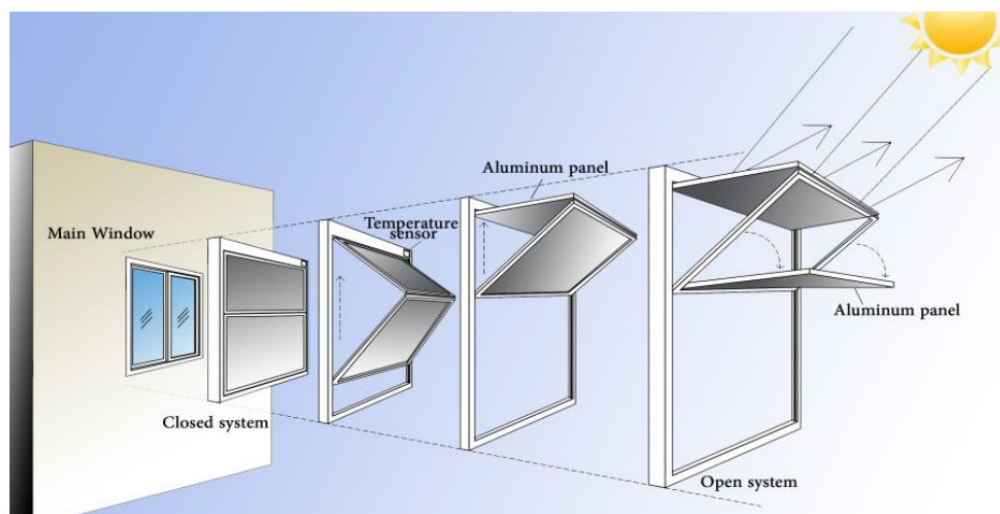


Figure 17. Different states of the fordable panels.

3.1.3 Electrochromic Glazing (EC Glazing)

Electrochromic glazing, also called EC glazing, is a commercially-available technology that is able to play both the roles of building enclosure as well as shading devices. The switchable tint of the glass pane (Figure 18) provides flexibility to the window's solar heat gain coefficient (SHGC) and visible light transmission (VLT).

Meanwhile, EC glazing provides an unblocked view to the exterior for the building occupants due to the absence of physical shading components including interior curtains, blinds and exterior louvers. A study conducted by M. Murphy et al. in Norway evaluated the energy-saving performance of EC glazing [20].



Figure 18. Range of tint of an electrochromic window.

The research was a computational simulation-based evaluation. The simulated model was set to a 1200-square-meter office building with the long wall orientated toward south. The EC glazing was applied to the southern, eastern, and western facades with 64.8% window to wall ratio, and the window assembly was triple pane glazing with one outer pane of EC glass and two inner panes of clear float glass with 90% Argon, 10% Air within the cavities.

The goal of this research was to evaluate different control strategies of the trigger of EC glazing's tint. Seven groups of the control strategies were simulated for the time period of a year (Table 6). In addition, two scenarios of different heating/cooling supplies, including district supply versus local heat pump, were simulated. It was concluded that the energy savings potential for the control strategies in relation to the fixed clear window ranged between 5,200 and 14,000 kWh per year, within which control strategies of zone temperature and incident solar energy operate better than the others.

- A Static Window – Clear ECW all year round
- B Static Window – Tinted ECW all year round
- C Switch governed by the incident solar radiation on the south facade
- D Switch governed by a time schedule
- E Switch governed by the outdoor ambient temperature
- F Switch governed by the outdoor ambient temperature during a set time frame and only on workdays
- G Switch governed by the operative temperature within the south thermal zone

Table 6. Control Strategies of the tint of EC glazing [20].

3.2 Complex Shading Models

3.2.1 Origami (Kaleidocycle Façade)

Origami is an ancient art that is made up of a set of paper-folding configurations. In the research conducted by Elghazi et al. [21], the authors examined the daylighting condition of a residential unit that has so-called Kaleidocycle Façade inspired by origami. A unit of Kaleidocycle is composed of a ring of tetrahedrons (Figure 19). By changing the rotation angle of tetrahedron on each side, the device will operate as an aperture providing control of the amount of penetrating light. Also, the diameter of the ring affect on the light penetration. Therefore, ring diameter (20 cm to 65cm, step 1cm) and rotation angle (0 to 90 degrees, step 1 degree) were the two variations for the device’s optimization process. The objective of optimization was to maximize the daylit area and to minimize the over-lit area in the study residential unit. The result shows that the optimized Kaleidocycle façade makes the residential unit perform better than the daylighting expectation of Leadership in Energy and Environmental Design (LEED) v4 and Daylight Availability. The indoor daylight quality meets sDA = 100% which is more than LEED v4 requirement of 75%. Annual Sun Exposure (ASE) is 5% which is two times less than LEED v4 requirement of 10%.

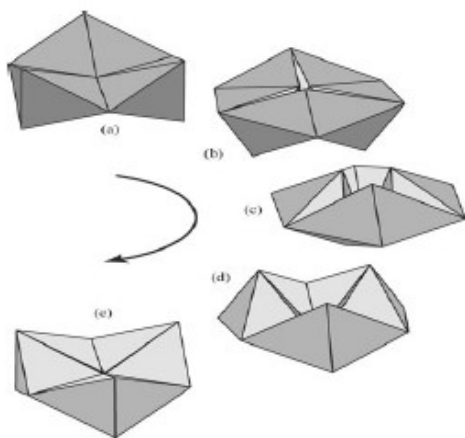


Figure 19. Kaleidocycle rotation motions.

3.2.2 Biomimetic Structure

A biomimetic strategy is a prevailing façade design approach. Research done by A. Jahanara et al. in Italy evaluated the performance of a lotus-like dynamic shadings on a south facing office building in Rome [22]. Inspired by vegetation’s innate behavior of interacting with the nature, the idea of the biomimetic strategy aimed to adopt the form of a plant to design a façade that can be transformed responsively to the lighting condition (Figure 20). By setting different “openness” of the lotus petals, i.e. fully open, partially open, and close as variables, and by establishing three different patterns of the device, the study tested out a wide range of possible shading configuration. Digital model built in Rhinoceros and lighting stimulation done by DIVA (a Solemma's legacy daylighting and energy modeling plug-in for Rhinoceros. The plug-in was initially developed at the Graduate School of Design at Harvard University and is distributed by Solemma LLC. [23], <https://www.solemma.com/Diva.html>) were used for the study. The criteria of Useful Daylight Illuminance (UDI) was adopted to evaluate the lighting condition. March 21st, June 21st, September 21st, and December 21st were the chosen dates for stimulation.



Figure 20. The proposed biomimetic geometry in Jahanara’s research.

The authors defined three levels for indoor illumination. The “daylit” area achieves illuminance levels between 100 lux to 2000 lux; “overlit” area achieves illuminance greater than 2000 lux with potential glare; and “partially-lit” area achieves illuminance below 100 lux. In summer, in the base case scenario (window without shading), nearly 50% of the floor area achieved “daylit”. However, the other 50% of the floor area was “overlit” with visual discomfort. On the other hand, in winter, less than half of the floor area was “daylit”, while the other half was divided into “overlit” and “partially daylit”. After the intervention of the proposed “blooming” shading system, the required daylight condition was achieved better than the base case: the “daylit” area percentage reached 99% of the space in June; the closed and the totally opened geometry gave the most appropriate “daylit” area. The partially opened geometry increased the “daylit” area to almost 100% in March and September.

3.2.3 Hexagonal Façade Skin

A study exploring hexagonal façade skin was conducted by Ayman H. A. Mahmoud et al. in Egypt [24]. The study aimed to design hexagonal façade pattern parametrically in Grasshopper. The parametric modeling strategy allows this study to generate diverse iterations of the geometry (Figure 21). The proposed hexagonal skin was operated in two ways: the first one is “rotation” in which the hexagonal unit rotates around its centroidal axis ranging from 30 to 165 degrees in 15-degree increments; the other one is “translation” in which the unit slides over the other. From close to fully open, the translation motion is divided into 10 steps. For comparison, three scenarios on a southern façade were simulated, i.e. 20% WWR punched window (as the base case), hexagonal façade skin with rotational motion, and hexagonal skin with translational motion.

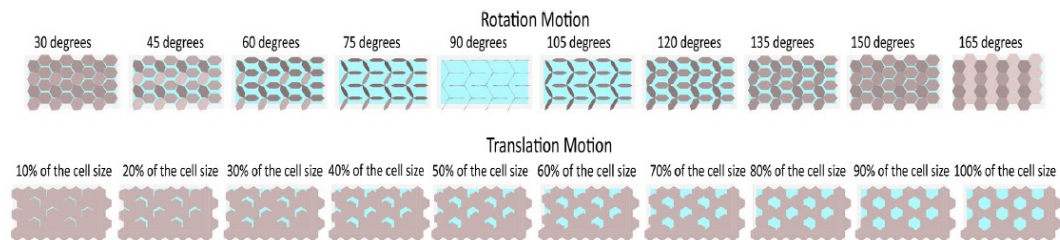

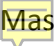


Figure 21. Two operational modes of the hexagonal pattern.

The result shows that both façades with rotation and translation motion skin have better daylight performance than the base case. In terms of the floor areas that fall into “daylit” illuminance level defined by  daylighting requirement (300 to 3000 lux), the rotational motion improved daylighting by approximately 50% in summer and spring versus approximately by 30% in autumn and winter compared to the base case. On the other hand, the translational motion improved daylighting by 50% in summer and spring while 20% in autumn and winter compared to the base case.

3.2.3 Shape Variable Mashrabiya (SVM)

A study conducted by L. Giovannini et al. in Abu Dhabi shows the performance of Shape Variable  (SVM) shading screen (Figure 22) in terms of saving energy for cooling and lighting [25]. Mashrabiya is a spiritual, decorative, and functional architectural element that merges the form and function of the Islamic window screen with a conventional jalousie, taking on the materiality of local culture [26].

An office building was set as the study model in Abu Dhabi where the climate is hot and arid. The variables in different scenarios are various shading devices, including

SVM with three different light reflectance, venetian blinds, and two different types of glazing, including double pane selective glass (visible light transmission, LT = 41%, solar heat gain coefficient, SHGC = 22%, thermal transmission, U-value = 1.1 W/m²K), and double pane reflective glass (LT = 16 %, SHGC = 19%, U-value = 1.1 W/m²K). The SVM screen is an adaptive shading and daylight control device consisting of three identical opaque backscattering shields that are carved with a pattern inspired by the local vernacular mashrabiya. By controlling the overlapping area between each layer of the shields, the SVM can be switched between fully closed and open position responding to the illuminance condition. For the external venetian blinds, two modes were created to simulate the users' behavior. The first one assumed that the occupants will actively open and close the venetian blinds corresponding to the daylight condition. The other assumed that the occupants tend to keep the blinds closed and work in electrical lighting.

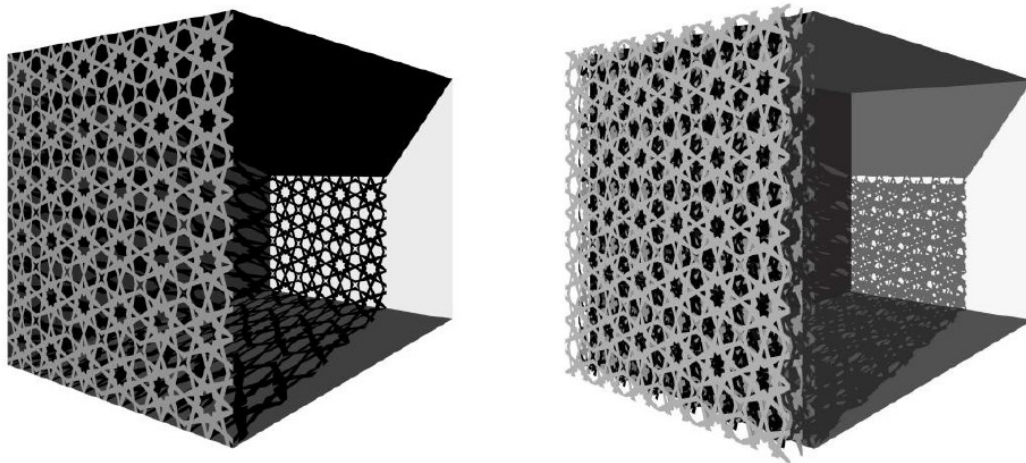


Figure 22. Shape Variable Mashrabiya (SVM).

Using 20°C (68°F) in winter and 26°C (78.8°F) in summer as the thermal comfort zone, the result of the study shows that SVM system reduces energy demand for cooling by 9.9% compared to venetian blinds and by 17.2% compared to double panel selective glazing (LT = 41%, SHGC 22%, U-value, 1.1. W/m²K). On the other hand, SVM system reduces energy demand for lighting by 30.7% lower than venetian blinds and by 65.7% lower than double pane reflective glazing (LT = 16%, SHGC = 19% and U-value = 1.1. W/m²K). The author concluded that the SVM system is able to reduce total energy consumption by 16.3% lower than venetian blinds and by 27% lower than double pane reflective glazing throughout a year.

Chapter 4: Methodology

This section describes my process for evaluating the energy-saving performance of

the designed dynamic shading screen. Considering the timeframe of this research, which eliminates the feasibility of long-term investigation in the actual environment, a simulation-based method is used to evaluate performance. Energy end-use model developed in Honeybee (a plug-in program for Grasshopper that supports detailed daylighting and thermodynamic modeling [27], <https://www.ladybug.tools/honeybee.html>) in Grasshopper (a visual programming language and environment that runs within the Rhinoceros, <https://www.rhino3d.com/en/6/new/grasshopper>[18]) is the adopted tool for the analytical work. To make the energy end-use model reflect the reality of housing typologies, construction materials, opening's orientation, and vacancy rate, etc., statistical data of residential buildings published by *Construction and Planning Agency Ministry of the Interior* [28], is used as the basis for the model inputs. To compare the energy-saving performance among different shading devices, energy end-use simulations were run through four scenarios: (1) no shading as the baseline, (2) static shadings (including overhang and louvers), (3) the proposed dynamic shading screen, and (4) always closed static shading. The results are shown graphically in the following section.

4.1 The Prototype of the Dynamic Shading Screen

Adapted from the existing window grilles, a prototype of the dynamic shading screen is modeled in Grasshopper (Figure 23). Since the model was built parametrically, the frame dimensions, the fin's operational directions (horizontal or vertical), and the fin's scale can be modified easily. In Figure 23, the dynamic shading screen is facing south. The motion of the rotatable fins is operated based on the illuminance level received on the fin's surfaces. As an initial setting, the fins will be fully opened at 7 am and 5 pm; they will be fully closed at noon; the fins' rotation angle will be increased incrementally from fully open to fully closed according to the received illuminance level.

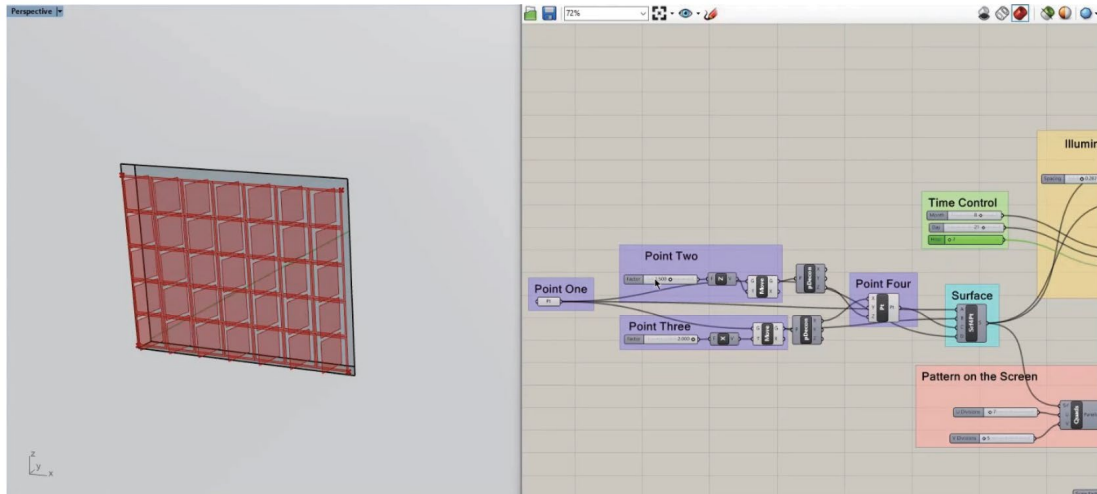


Figure 23. A prototype of a dynamic shading screen adapted from the window grilles.

4.2 Settings in Computational Simulation

4.2.1 Housing Typologies

Based on the statistical data in *National Residential Buildings Survey* (Figure 24), apartment/condo and townhouse are the most dominant housing typologies in the country, which account for 32.1% and 34.58% respectively [28]. In sum, apartment/condo and townhouse represent 66.7% of all housing types in Taiwan. Accordingly, these two types of housing are the targets built in the Honeybee energy model.

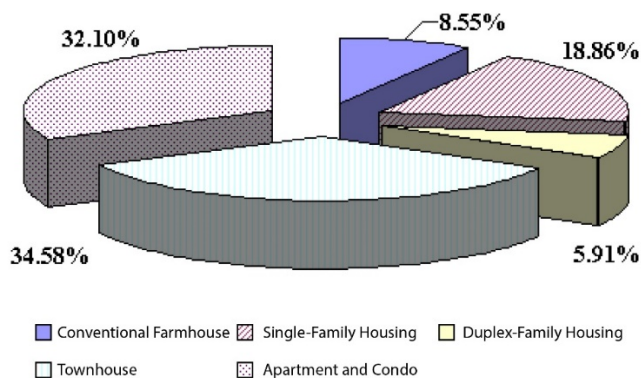


Figure 24. The percentage of different housing types in Taiwan published by *Construction and Planning Agency Ministry of the Interior* [28].

4.2.2 Solar Radiation Intensity Test

To determine the target orientation for simulation in the energy model, a solar radiation intensity test is conducted in DIVA (a Solemma's legacy daylighting and

energy modeling plug-in for Rhinoceros. The plug-in was initially developed at the Graduate School of Design at Harvard University and is distributed by Solemma LLC. [23], <https://www.solemma.com/Diva.html>). The mean solar radiation gained by each orientation is summarized in Table 7. Eastern, Western, and Southern surfaces gain the most solar radiation throughout a year in Taiwan. As such, in the Honeybee energy model, those three orientations will be used to test the shading systems.

Orientation	Mean Solar Radiation in a Year (kWh/m ²)
East	600.9
West	571.5
North	325.7
South	648.4

Table 7. Mean solar radiation gained by each orientation.

4.2.3 Energy Model of An Apartment

To represent an apartment in Honeybee, a single-zone study model of 144 m² (12m x 12m) (1,550 ft²) was built. An apartment unit typically occupies the corner of a floor plate with two walls facing the exterior and two remaining walls facing the inner circulation space or the wall of the neighbor. Accordingly, the study unit has two exterior (diabatic) walls and adiabatic walls (connected to adjacent unit or facing the hallway). Each exterior wall has two openings set to the dimension of 1.5m x 1.8m with 0.9m sill height.

The construction type of wall and the glazing type are determined based on climate zone. To reflect the climate in Taiwan, climate zone 2 in the U.S. (Figure 25) is used as the basis for construction assemblies set for the simulation.

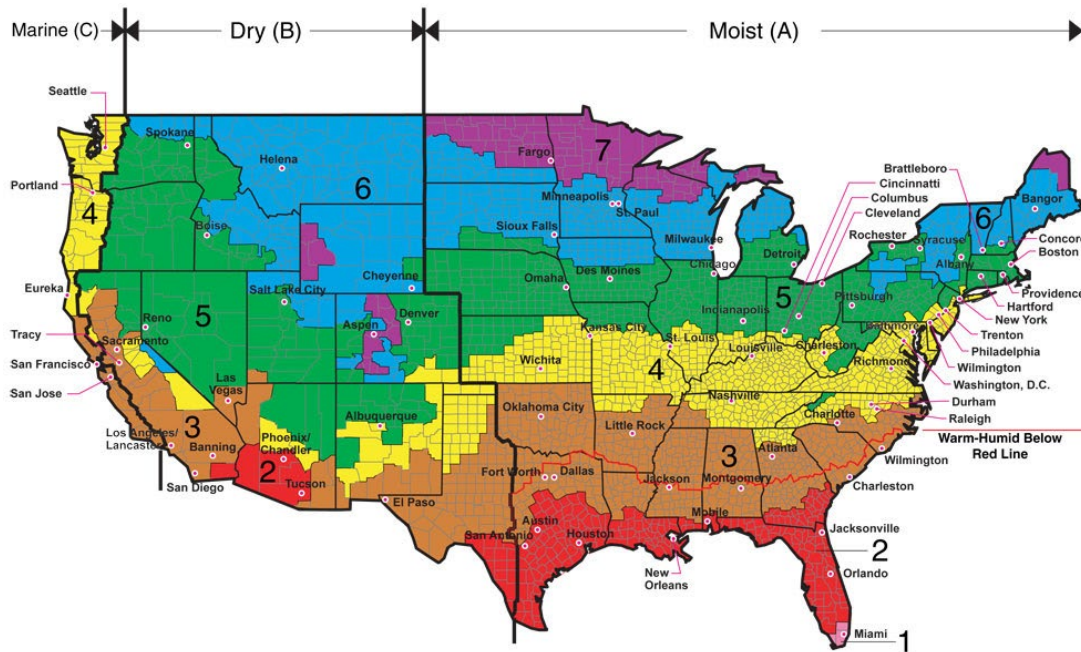


Figure 25. Climate zone in the U.S. defined by the American Society of Heating, Refrigerating and Air-Conditioning Engineers (ASHRAE) [29].

To closely reflect the uses of AC, lighting, and equipment in the energy model, the settings in the apartment’s energy model are summarized in Table 6. Cooling set point is set at 27°C (80.6°F) determined by the temperate at which air condition is needed. The cooling set back is set at 50°C (122 °F) to ensure the air conditioner is turned off without occupants in the building. The lighting illuminance set point and the lighting density are set to 300 lux and 3 W/m² to meet the needs of reading and writing on paper in the indoor spaces. The equipment load is set at 5 W/m² to reflect the energy consumption summarized in Table 6. Number of people per area is set at 0.027 ppl/m² derived from the calculation of four people dwelling in a 144 m² apartment. The infiltration rate is set at 0.0003 m³/S m² as an average rate without leaking defined by the American Society of Heating, Refrigerating and Air-Conditioning Engineers (ASHRAE).

Category	Settings
Square footage	144 m ²
Number of floors	1
Orientation of diabatic walls	West and south
Cooling Set Point	27°C (80.6°F)
Cooling Set Back	50°C (122 °F)
Lighting Illuminance Set Point	300 lux
Lighting Density Per Area	3 W/m ²
Equipment Load Per Area	5 W/m ²
Number of People Per Area	0.027 ppl/m ²
Infiltration Rate Per Area	0.0003 m ³ /S m ²

Table 8. The settings in the apartment energy model.

4.2.3 Energy Model of a Three-story Townhouse

In this scenario, a three-zone study model of 252 m² (2,713 ft²) (14 m x 6 m each floor) is built to represent a three-story townhouse. Considering the typical configuration of townhouses and the result of the solar radiation intensity test, the study unit has two exterior walls on its transverse sides and two adiabatic walls on its longitudinal sides. Each exterior wall on each floor has one opening set to the dimension of 1.5m x 1.8m with 0.9m sill height, except a larger one (1.8m x 2.1m) in the ground floor representing the opening in the living room.

The settings for cooling, lighting, equipment, etc. are the same as the ones in the apartment scenario except the equipment load is lowered to 3 W/m² to reflect the more scattered distribution of equipment in the three-story building. Number of people per area is set to 0.015 derived from the calculation of 4 people dwelling in a 252m² townhouse. The settings are summarized in Table 7 below.

Category	Settings
Square footage	252 m ²
Number of floors	3
Orientation of diabatic walls	North and south
Cooling Set Point	27°C (80.6°F)
Cooling Set Back	50°C (122 °F)
Lighting Illuminance Set Point	300 lux
Lighting Density Per Area	3 W/m ²
Equipment Load Per Area	3 W/m ²
Number of People Per Area	0.015 ppl/m ²
Infiltration Rate Per Area	0.0003 m ³ /S m ²

Table 9. The settings in the townhouse energy model.

4.3 Calibration of the Energy Models

Calibration of the energy models is crucial for the simulation process to ensure that baseline models are reflective of typical energy use patterns of these building types in Taiwan. A comparison between the energy consumption derived from the estimation done by this research and the energy consumption derived from Honeybee simulation is made to verify the accuracy of the simulation (Figure 26). Comparing the proportion and the number of the energy consumption by sectors among cooling, lighting, and equipment, it is clear that the developed energy model is able to reflect the energy use conditions typically seen in these building types.

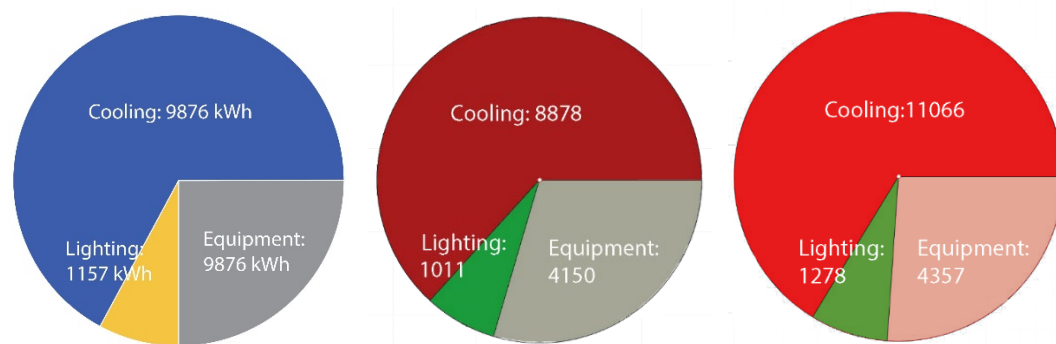


Figure 26. Pie chart on the left, the estimation of annual electricity consumption done by this research. Pie charts in the middle and on the right, electricity consumption derived from the energy models of the apartment and the three-story townhouse respectively.

4.4 Variables in the Simulation

The annual electricity consumption per household is simulated separately for the apartment and the townhouse. Orientations are assigned differently according to the housing typology and its layout (Figure 27). In the townhouse scenario, since windows are usually on both ends of the house, openings are assigned to east and west versus north and south. For the apartment, since a unit is usually layout at the corner of a floor plate, openings are assigned to east and south versus west and south.

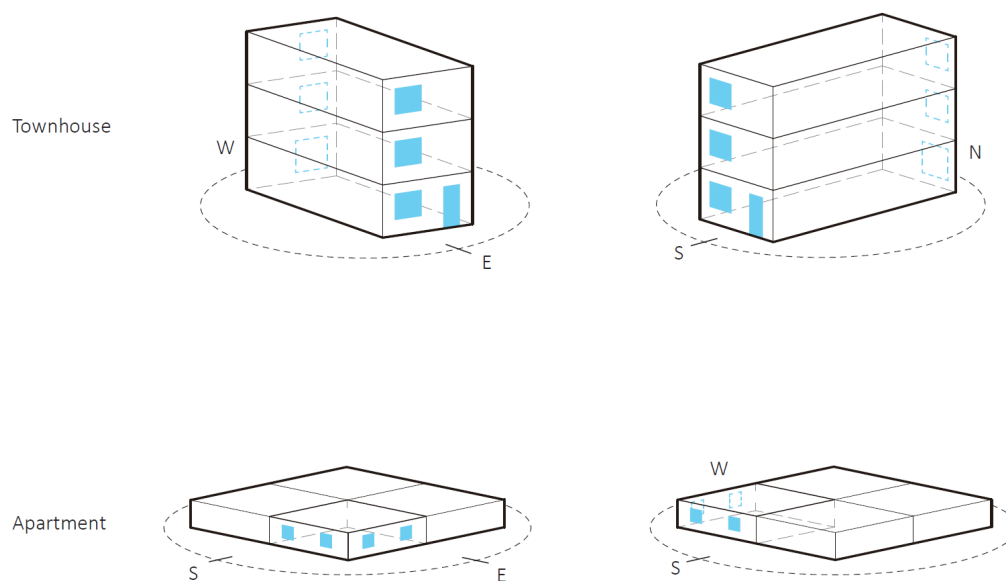


Figure 27. Orientations assigned to the townhouse and the apartment.

A tree diagram (Figure 28) illustrates all the testing variables in the simulation. Beyond the variables of housing typologies and orientations mentioned previously, a “set” of different shading strategies is grafted (the orange block in Figure 28). The testing strategies in the set range from an opening with no shading, a static shading system (include overhang and louvers), a dynamic shading system with different operational directions and pattern densities, to an always closed static shading system. The operational directions within the branch of dynamic shading screen, including horizontal, vertical, and mixed, determined the rotation directions of the rotatable fins. The “mixed” mode of the operational direction adopts the commonly used shading strategy [30], horizontal baffles for the south versus vertical fins for the east/west. However, the mixed mode is not applicable for the townhouse due to its orientation. Ultimately, thirty-six scenarios were run in the simulation. In terms of materiality, the materials of the static shading devices (overhang and louvers) and of the always closed static shading are opaque, non-reflective panels; the material of

the dynamic shading screens is translucent panels with 20% visible light transmission (VLT).

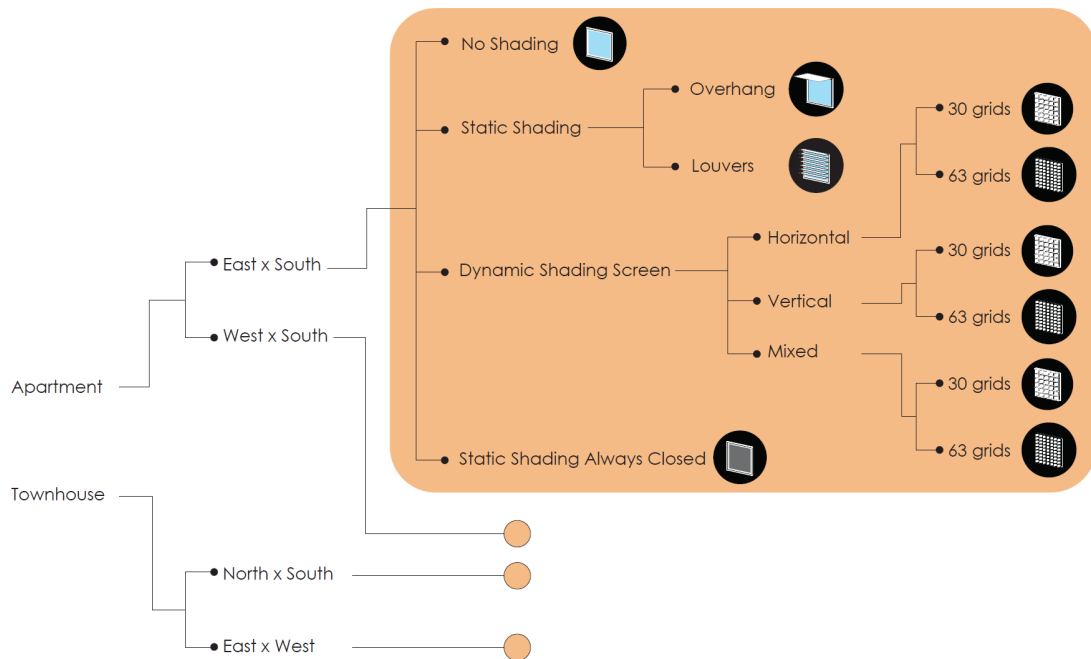


Figure 28. A tree diagram of variables in the energy end-use simulation.

Chapter 5: Results

1.1 Results from the Townhouse Model

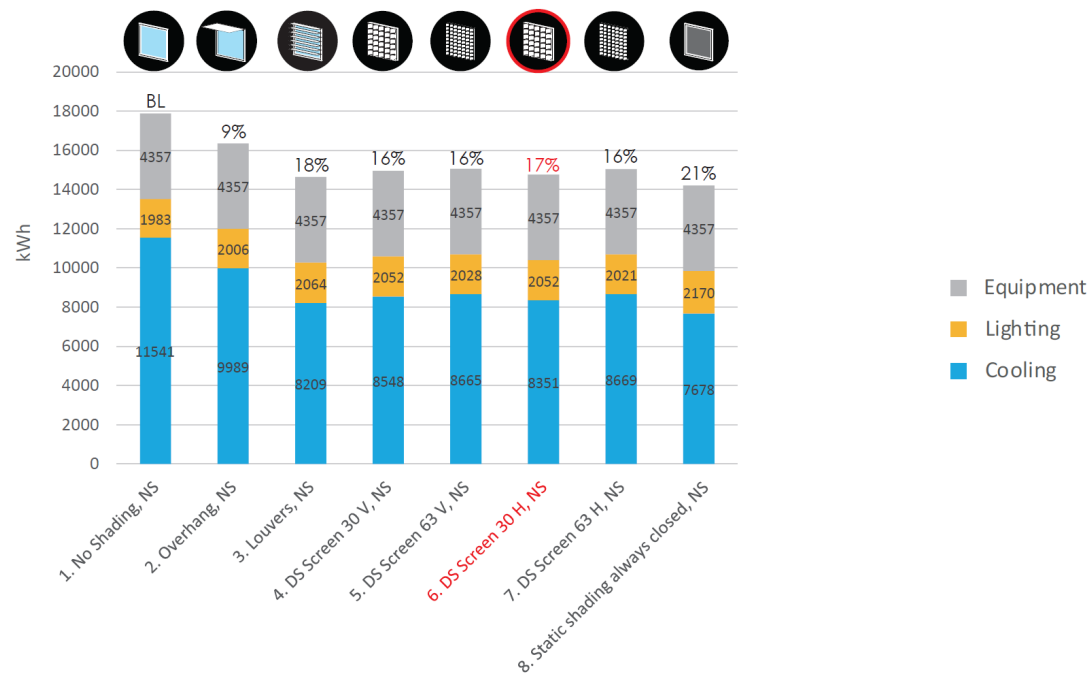


Chart 1. Electricity consumption in Townhouse. Orientation: north south.

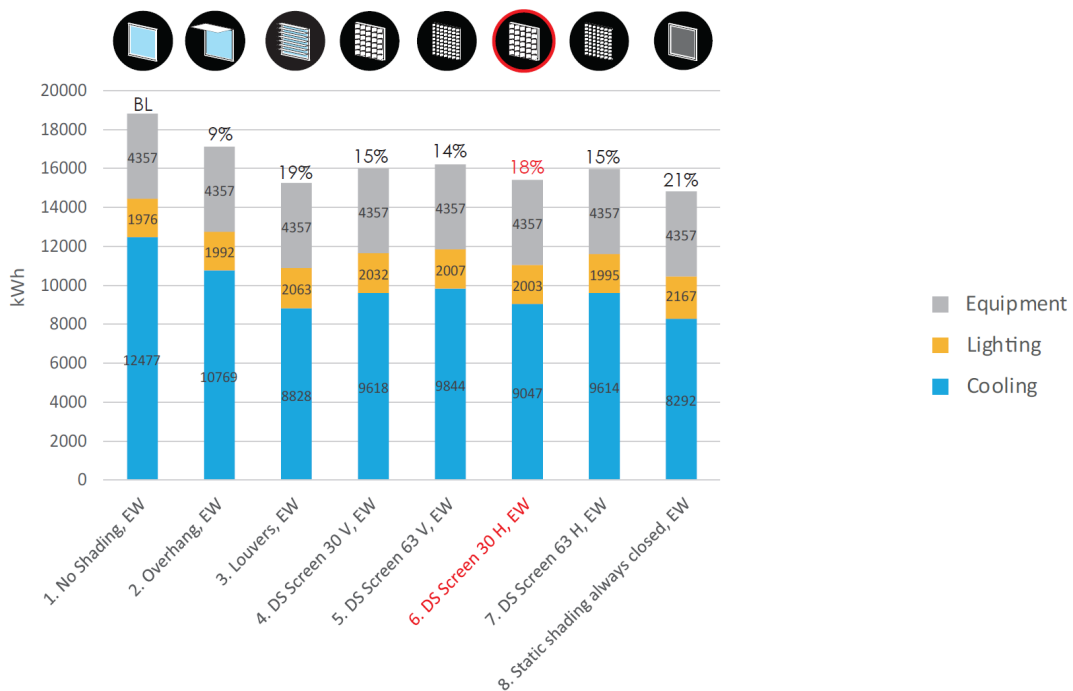


Chart 2. Electricity consumption in Townhouse. Orientation: east west.

Chart 1 shows the electricity consumption in the townhouse facing north and south with all the tested shading devices. Since the “no shading” scenario consumes the most electricity, it is set as the baseline. The static shading always closed scenario performs the best from an energy standpoint, which provides 21% energy saving compared to the baseline. Louvers and overhang save 9% and 18% respectively compared to the baseline. Among the dynamic shading screen scenarios, the run with larger rotatable fins and the horizontal operational direction performs better than others, which save 17% energy compared to the baseline.

Similar energy-saving performance pattern can be seen in the townhouse with the orientation of east and west (Chart 2): static shading always closed scenario save the most energy (21% compared to the baseline); louvers performs two-times better than overhang (19% and 9% respectively); the dynamic shading screen with the horizontal operational direction and larger rotatable fins performs better than the other dynamic shading screens (18% compared to the baseline).

1.2 Results from the Apartment Model

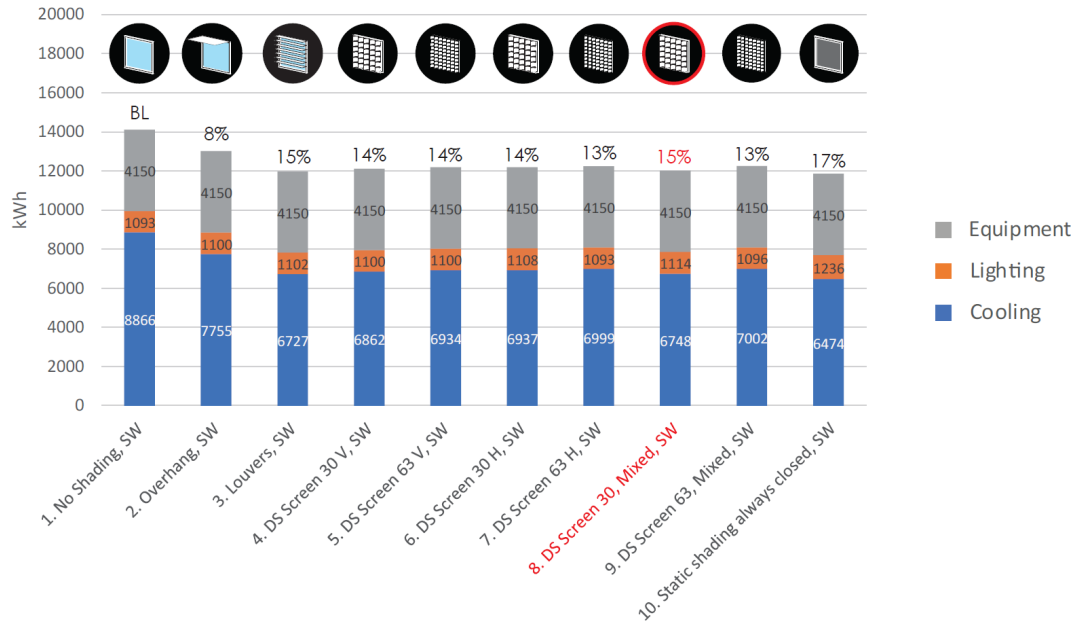


Chart 3. Electricity consumption in Apartment. (Orientation: south west).

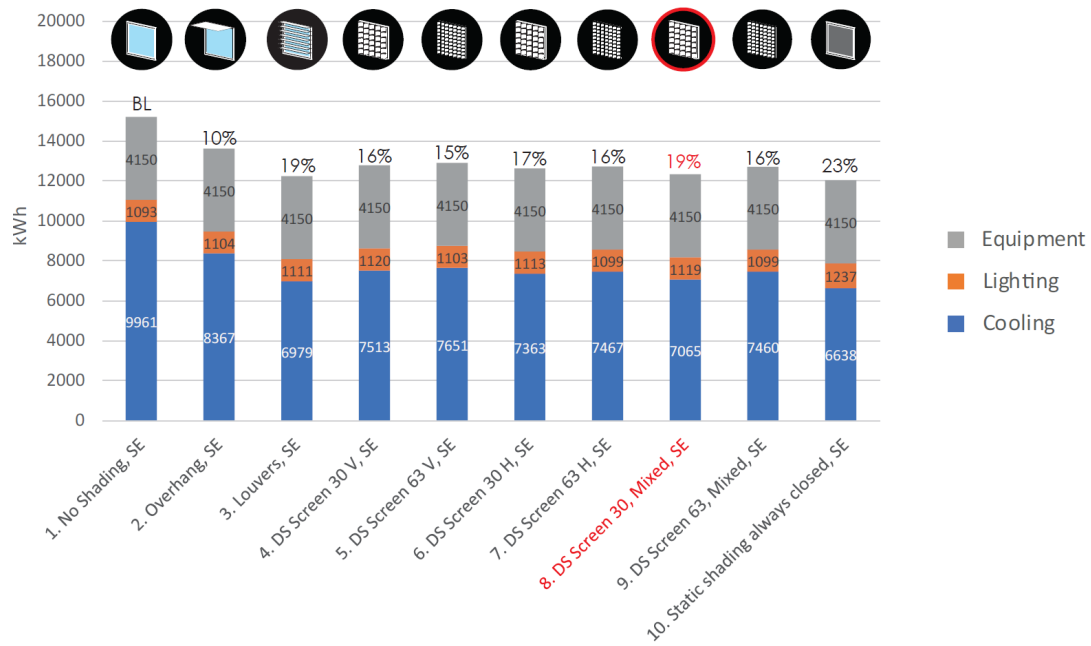


Chart 4. Electricity consumption in Apartment. (Orientation: south east).

In the apartment testing, similar the energy-saving performance pattern shown in the townhouse can be seen (Chart 3 and 4). For example, in the apartment with the orientation of south west, the static shading always closed scenario performs the

best (17% energy saving compared to the baseline); louvers perform two-times better than overhang (15% and 8% respectively compared to the baseline); the dynamic shading screen with the mixed operational direction and the larger rotatable fins performs better than other dynamic systems (15% energy saving compared to the baseline). Similar results can also be seen in the orientation of south east again

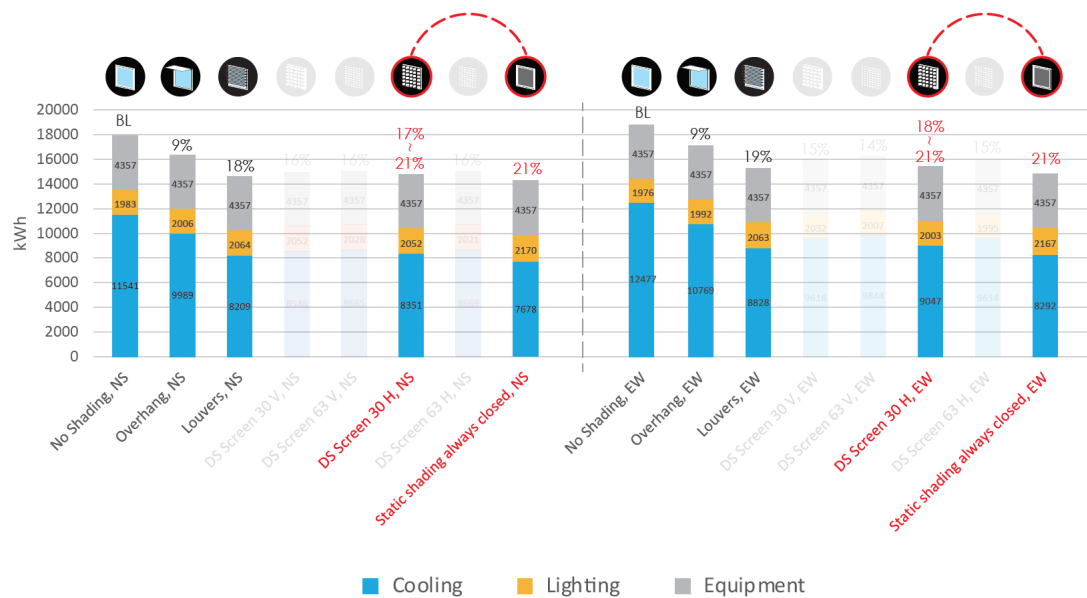


Chart 5. Summary of electricity consumption in the townhouse.

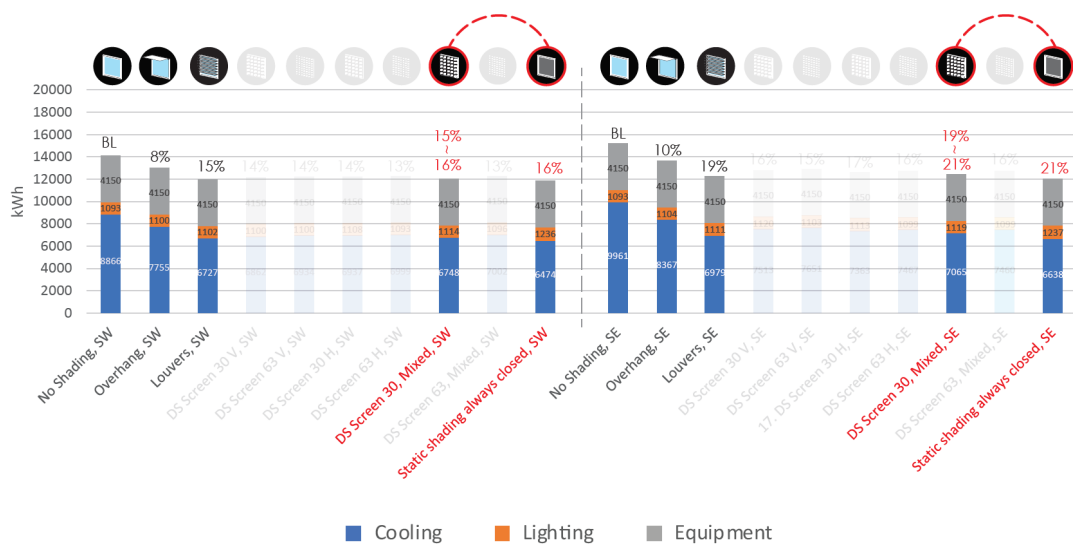


Chart 6. Summary of electricity consumption in the apartment.

Since all the dynamic shading screens were simulated in their fully open state (all rotatable fins are perpendicular to the frame), the percentages shown in Chart 1 to 4 are the dynamic shading screens' worst energy-saving performance. If the dynamic shading screens' rotation could be simulated in Honeybee, their energy-

saving performance in percentage would fall in the range between runs of their fully open state and the run of static shading always closed (Chart 5 and 6).

Chapter 6: Visualization

6.1 Visualization of an Apartment

In this chapter, a façade design on a new build mid-rise apartment is explored (Figure 29). A new-build residential building project is an opportunity to integrate the proposed dynamic shading screen with the building façade. Rather than regarding the dynamic shading screen as an attachment on the building's exterior, the proposed façade design aims to make the dynamic shading screen a feature that enriches the building's exterior characteristic by reviving the value of the traditional window grilles while reducing the building's peak cooling loads and improving the indoor thermal and visual comfort.



Figure 29. A façade design that could be used to integrate the dynamic shading screen with a mid-rise apartment.

Based on the results shown in the bar charts in Chapter 5, the dynamic shading screen with the mixed mode operation and larger rotatable fins performs better than the other configurations. Accordingly, the best performing configuration of the dynamic shading screen is applied to the apartment. To visualize the application and operation of the dynamic shading screen throughout a day, a series of renderings is made at different time spot. In the scene, the apartment façades integrated with the dynamic shading screen are facing east and south (Figure 30). The rotatable fins on the eastern façade rotate vertically while the fins on the southern façade rotate

horizontally in order to implement the mixed mode operation.



Figure 30. Orientation of the designed apartment.

Starting from 7 am, all the rotatable fins on both sides are in their fully open state because of the gentle sunlight intensity (Figure 31). At 10 am, when the sun rises up and the sunlight starts to hit the eastern façade, the fins on the east close 30 degrees (Figure 32). At 12 pm, when the sun reaches the zenith, fins on both east and south close 60 degrees to reduce solar heat gain (Figure 33). At 1 pm, when the sun starts to cause glare issue and radiate heat on the southern façade, the fins on the south fully close. Since the eastern façade has less direct sunlight at this time, the fins start to reopen (Figure 34). At 3 pm, when the sun moves to the west, fins on both east and south start to return to their open state (Figure 35). Finally, at 5 pm, all fins are back to their fully open state because of dimmer sunlight at dusk (Figure 36).

Although the operation of the dynamic shading screen is programmed to rotate automatically in response to the illuminance level received on the screen's surfaces, the occupants are still able to operate the screen depending on their needs or preference. Figure 32 and 35 illustrate the operational diversity among different apartment units. By providing operational flexibility to the occupants, the building may have a vivid appearance attribute to the diverse usage patterns.



Figure 31. Apartment with dynamic shading screens at 7 am.



Figure 32. Apartment with dynamic shading screens at 10 am.



Figure 33. Apartment with dynamic shading screens at 12 pm.



Figure 34. Apartment with dynamic shading screens at 1 pm.



Figure 35. Apartment with dynamic shading screens at 3 pm.



Figure 36. Apartment with dynamic shading screens at 5 pm.

6.2 Visualization of a Townhouse

Compared to the numbers of new build projects, there are more existing residential buildings in the country, to which the façade design proposed in the previous paragraph is not applicable. Therefore, for existing residential buildings, a façade renovation is proposed in this section (Figure 39).

To address this, a set of modular dynamic shading screens are envisioned to be installed outside the windows of residential buildings by manufacturers. The set

includes the components of window grille with rotatable fins mounted as the shading portion and a piece of PV panel plus a battery that drive the in-built motors as the power source (Figure 37). In order to provide diverse options to suit the house owners' preference or to match the architecture's characteristic, for both the frame and the rotatable fins, different patterns, materials, colors, and textures are provided (Figure 38).

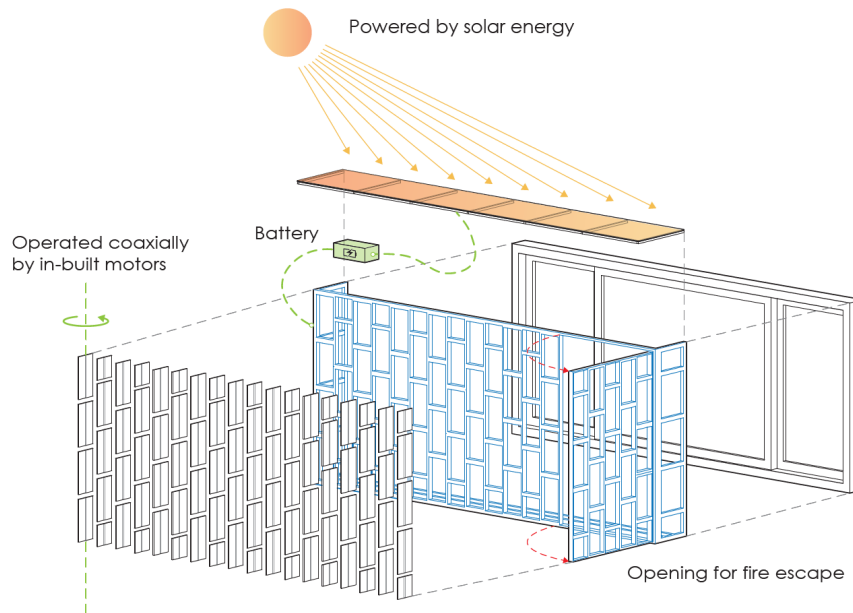


Figure 37. A set of dynamic shading screen that can be installed on an existing residential building.

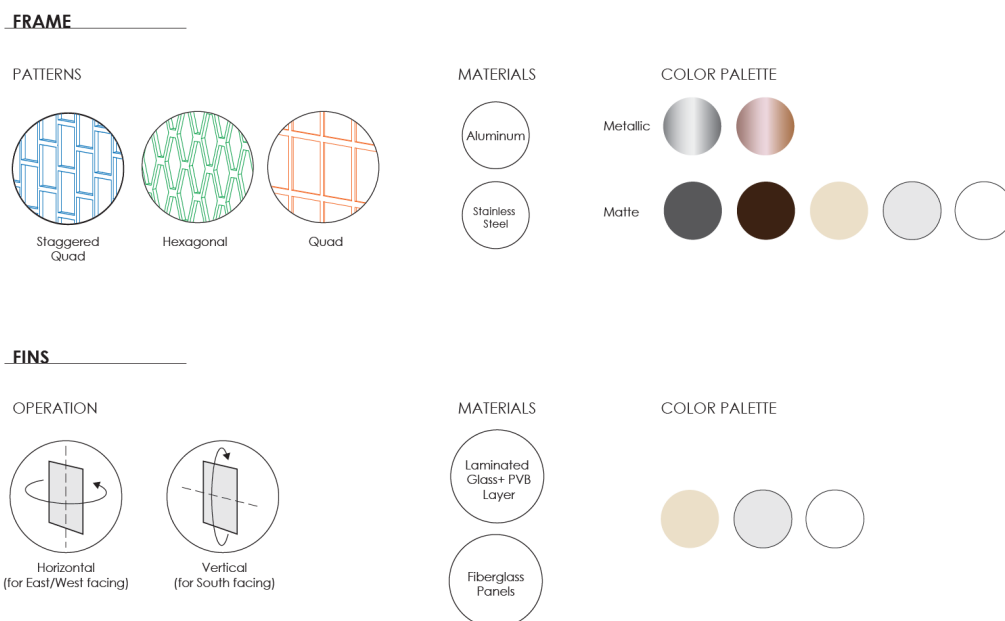


Figure 38. Options of the frames and fins.

To visualize the application and operation of the dynamic shading screen on an existing residential building, a series of renderings that represents typical townhouses in Taiwan is made at different points in time. In the scenes below, the row of townhouses on the right are facing west; the row of townhouses on the left are facing east. The observer is looking toward north when viewing the image (Figure 40).



Figure 39. The application of dynamic shading screen on an existing townhouse.



Figure 40. Orientation of the townhouse.

At 10 am, the sun is behind the right row townhouses. Since the façades of the right

row townhouses are in shade, all the rotatable fins are in their fully open state (Figure 41). At 12 pm, when the fins receive higher illuminance, they close 30 degrees to reduce the indoor solar heat gain (Figure 42). At 1 pm, when the sun moves to the west, the fins close 60 degrees to block the direct sunlight (Figure 43). At 3 pm, when more direct sunlight hit the western façade of the townhouse, the fins fully close to mitigate the solar heat gain and glare issue (Figure 44). At 4 pm, the sun moves to the back of the left row townhouse and cast shadow on the right row townhouse. At this moment, the fins on the second floor return to their fully open state while the fins on the third floor are still in their 60-degree-closed state due to the illuminance the fins receive (Figure 45).



Figure 41. The townhouse with dynamic shading screens at 10 am.



Figure 42. The townhouse with dynamic shading screens at 12 pm.



Figure 43. The townhouse with dynamic shading screens at 1 pm.



Figure 44. The townhouse with dynamic shading screens at 3 pm.



Figure 45. The townhouse with dynamic shading screens at 4 pm.

6.3 Visualization of Townhouse Interior

The main beneficiary of shading devices in residential buildings is the occupant experience. If the shading devices are well designed, the interior spaces will have better daylighting quality, thermal comfort, and energy use efficiency. In this section, a comparison of daylight quality with/without the dynamic shading screen in a townhouse's living room is visualized through a series of renderings at different times in a day. As mentioned in Chapter 4.4, the material of the dynamic shading screens is translucent panels with 20% visible light transmission.

For comparison, two renderings at the same point in time are put in juxtaposition. The dynamic shading screen on the left rendering will be in its fully open state throughout a day; the dynamic shading screen on the right will be operated in response to the sunlight. The window in the rendered scene is facing west so that the daylight will be changing along with the sun's movement. From Figure 46 to 51, it is clear to see the shading effect attributed to the dynamic shading screen, especially in the afternoon when the sun moves to the west and starts to irradiate the space through the window. As shown in Figure 50 and 51, when direct sunlight penetrates deeply into the space, the dynamic shading screen is able to block the sun beam and diffuse it into the interior without high contrast. With this shading operation, the space is well-daylit while avoiding glare and overheating.

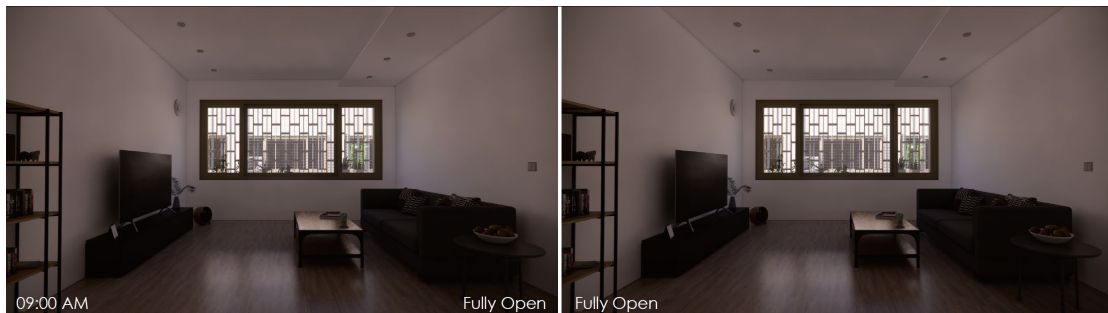


Figure 46. The interior of a townhouse with dynamic shading screens at 9 am.

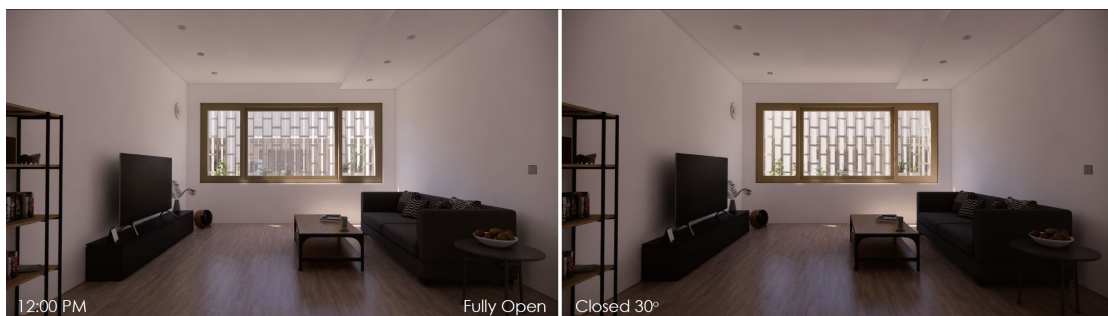


Figure 47. The interior of a townhouse with dynamic shading screens at 12 pm.

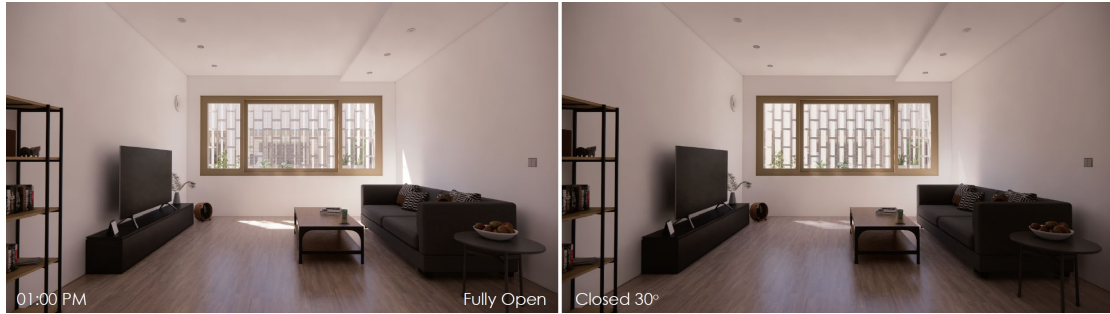


Figure 48. The interior of a townhouse with dynamic shading screens at 1 pm.

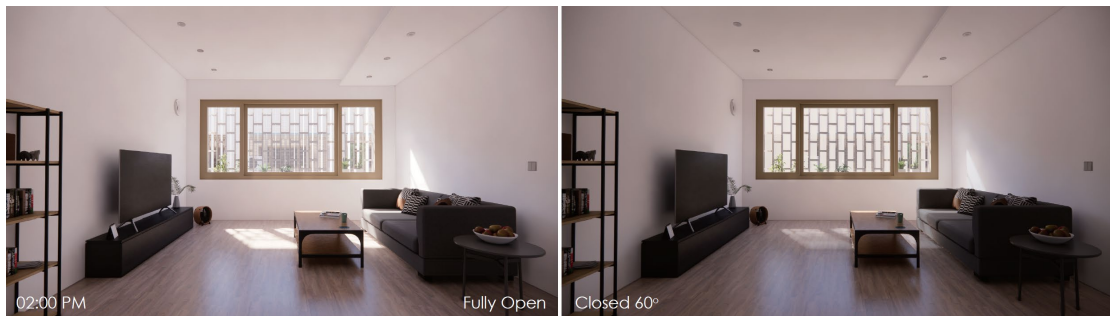


Figure 49. The interior of a townhouse with dynamic shading screens at 2 pm.

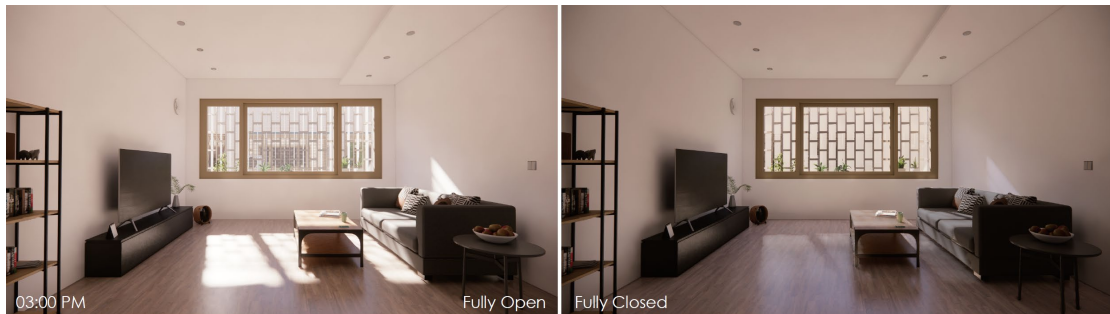


Figure 50. The interior of a townhouse with dynamic shading screens at 3 pm.

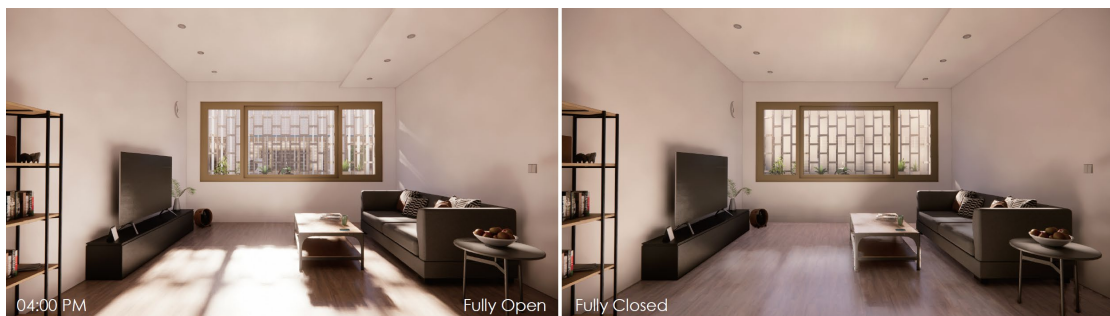


Figure 51. The interior of a townhouse with dynamic shading screens at 4 pm.

At 5 pm, when the sun is blocked by the adjacent building, the dynamic shading screen returns to its fully open state (Figure 52). At night, when no sunlight is

received, occupants can control the dynamic shading screen depending on their needs. They can either open the screen to have the outdoor view or close the screen to have more privacy (Figure 53 and 54).

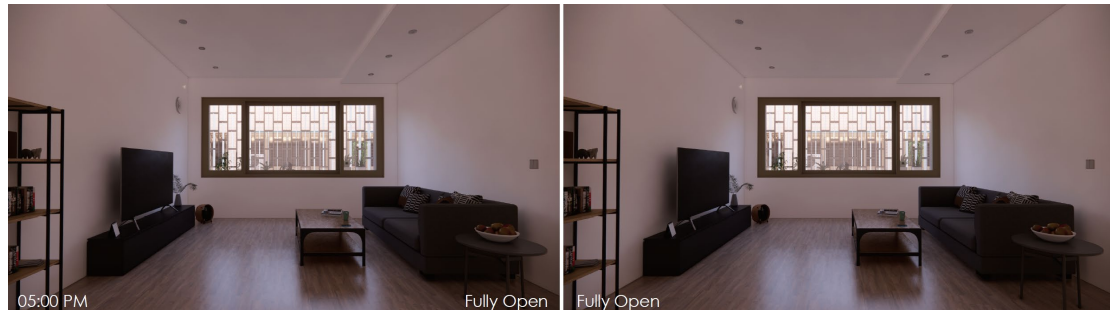


Figure 52. The interior of a townhouse with dynamic shading screens at 5 pm.

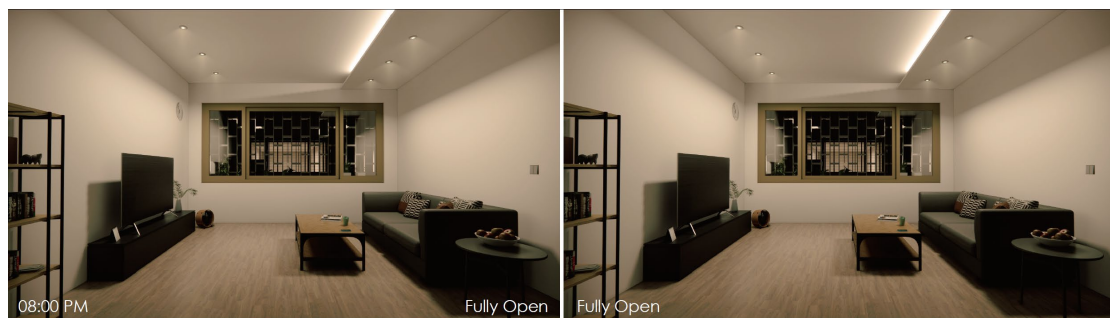


Figure 53. The interior of a townhouse with dynamic shading screens at 8 pm.

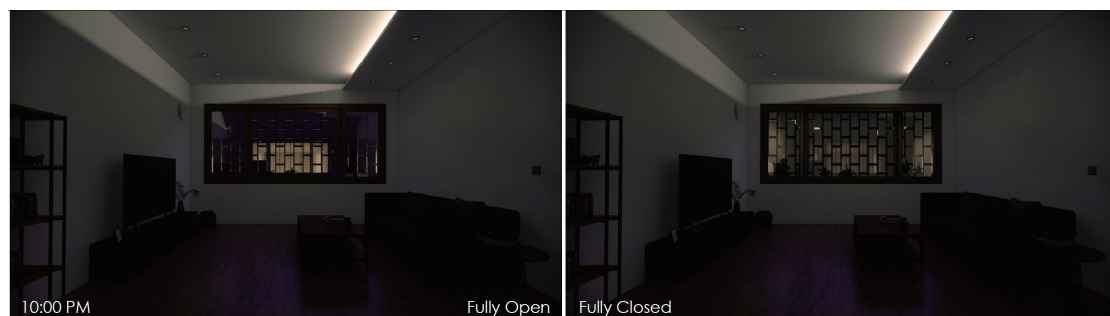


Figure 54. The interior of a townhouse with dynamic shading screens at 10 pm.

Chapter 7: Luminance and Illuminance Testing

7.1 Introduction

To further assess the daylight performance of the dynamic shading screen through a qualitative lens, a building sectional luminance distribution, point-in-time illuminance range, and annual illuminance testing were conducted. The model used is the townhouse shown in the previous chapter (Figure 55).



Figure 55. The testing townhouse.

7.2 False-Color Luminance Distribution

For the luminance-based analysis, a section is cut through the townhouse's longitudinal direction, east-west direction in this case (Figure 56 left). The study space is the townhouse's second floor which can be divided into three portions based on the typical uses (Figure 56 right). The spaces on the two ends (next to the eastern and western windows) are the primary and secondary occupiable spaces. Typically, living room/dining room and bedrooms will be assigned to these spaces. The area in the middle (next to the stair) is typically used for circulation and utility space. Hallway, bathroom, and storage zones are usually assigned to this space. Based on this spatial hierarchy, the simulation and analysis will be focused on the two occupiable spaces.

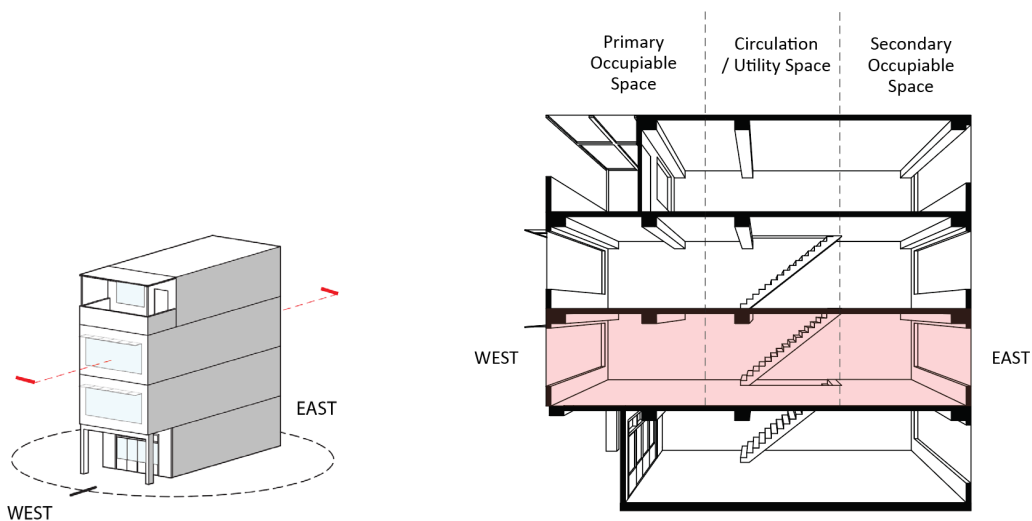
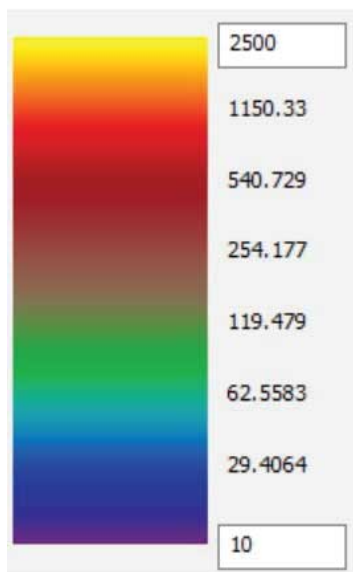


Figure 56. A section cut of the townhouse.



False-color is the adopted measure to visualize the result of luminance distribution. The range from 10 to 2500 is set so that green in the middle of the measure will be representing the well-lit condition; yellow will be representing over-lit condition; purple will be representing poor-lit condition (Figure 57). The variables in the simulation are two sky conditions (overcast and clear sky with sun), three dates (June 21st, September 21st, and December 21st), and three points in time (9 am, 12 pm, and 4 pm). For comparison, the scenario of no shading on both eastern and western windows is set as the baseline which is listed in the left column in the following figures.

Figure 57. False-color luminance scale.

The operational logic and the material (translucent panel with 20% VLT) of the dynamic shading screen is the same as the one described in the previous chapters. The fins' rotation angles will be determined based on the illuminance level received on the fins' surfaces. In Figure 58 to 60, it is noticeable that generally with the dynamic shading screen, the over-lit areas shown in the baseline are either reduced or transformed to green and blue colors (in the false-color images) in the two occupiable spaces, especially at 9 am and 4 pm when the spaces receive significant direct sunlight. The only drawback caused by the dynamic shading screen occurs when the sky condition is overcast. The interior with the shading screen may be dimmer than the interior of the baseline. Shade screen sensors could be programmed to revert to the fully opened state under overcast conditions to mitigate this condition if desired. However, sky condition in Taiwan is clear sky with sun in most of a year. Overcast sky occurs only during the rain season in May.

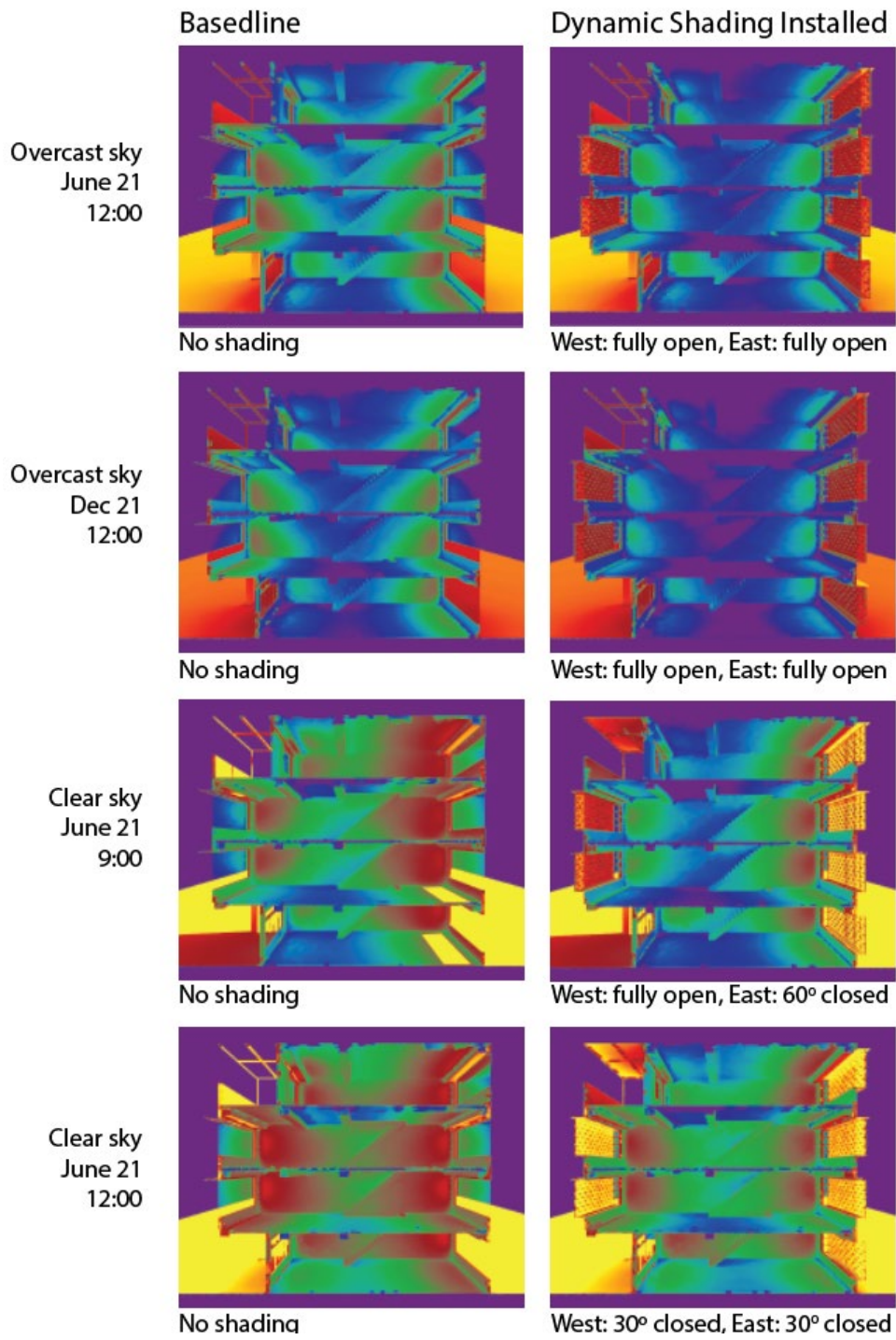


Figure 58. False-color luminance distribution A.

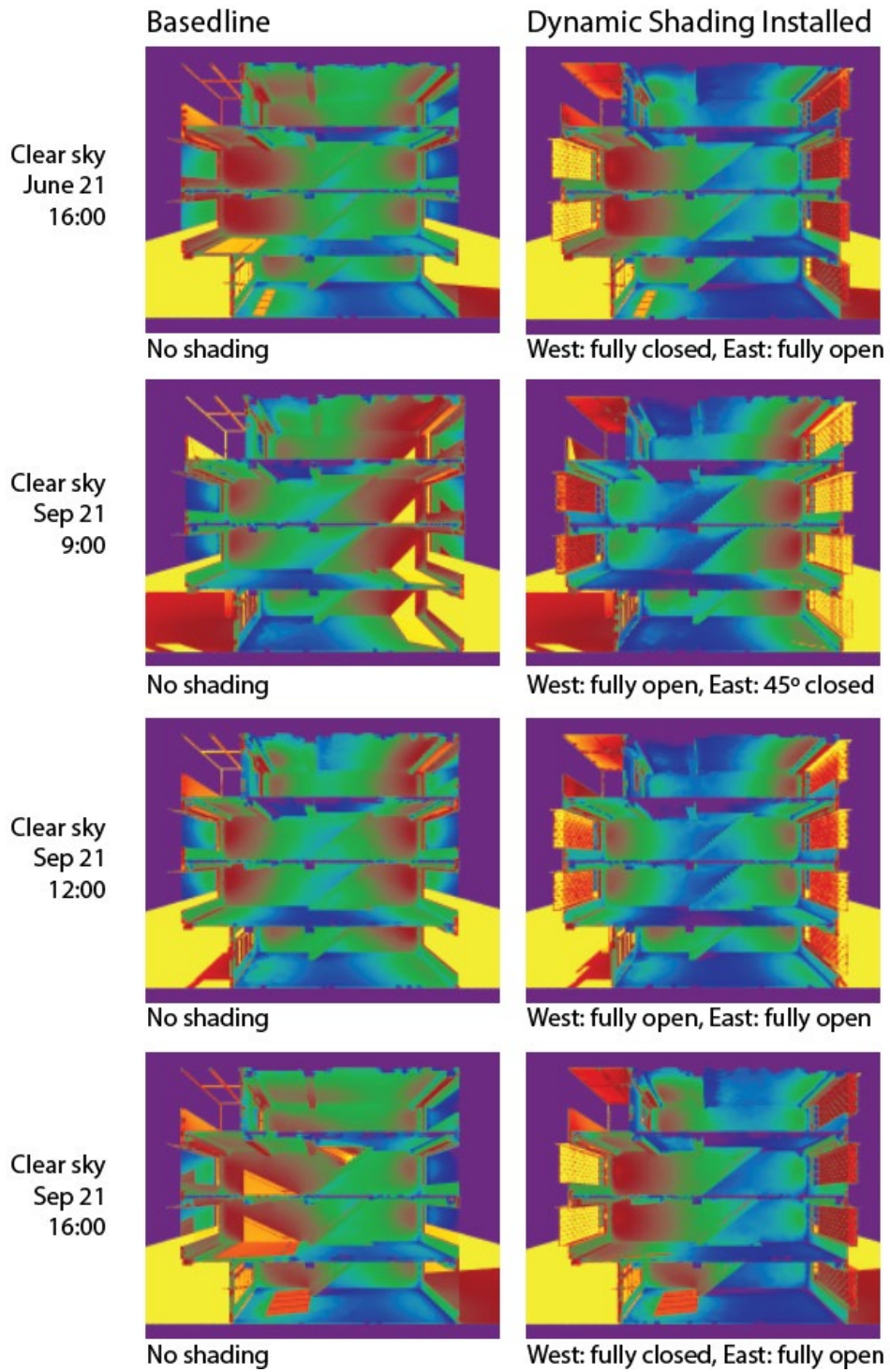


Figure 59. False-color luminance distribution B.

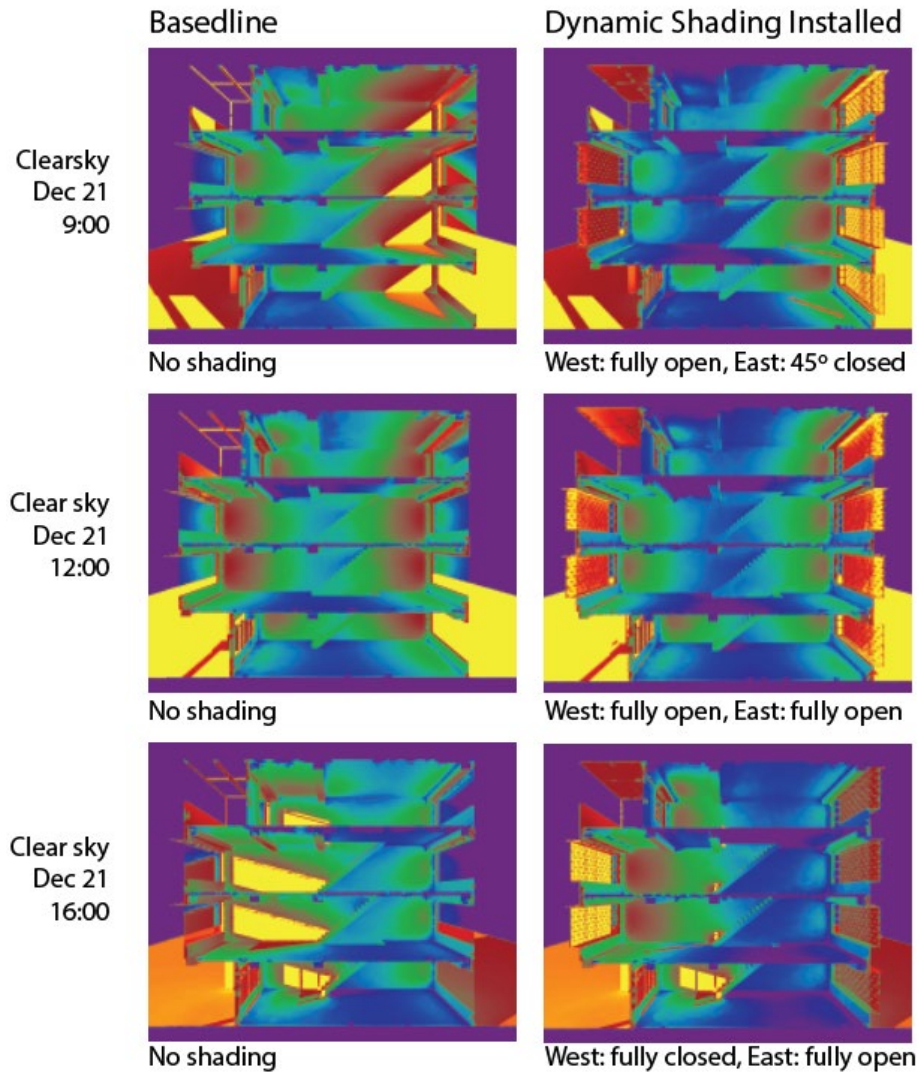
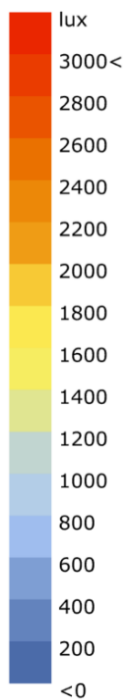


Figure 60. False-color luminance distribution C.

7.3 Point-In-Time Illuminance Range



In this section, a grid-based, point-in-time illuminance analysis is conducted. This is to quantitatively evaluate the intensity of light within the space at key points in time. The variables are the same as those in the false-color luminance testing: two sky conditions (overcast and clear sky with sun), three dates (June 21st, September 21st, and December 21st), and three points in time (9 am, 12 pm, and 4 pm). The lowest and the highest boundaries of the measure are set to 0 lux and 3,000 lux respectively (Figure 61). Target lux levels are from 100 – 3000 lux. For comparison, a scenario of no shading on both eastern and western windows is set as the baseline which will be listed in the left column in the following figures. The operational logic and the material (translucent panel with 20% VLT) of the dynamic shading screen are the same as the ones mentioned in the previous chapter. The fins' rotation angles will be determined based on the illuminance level received on the fins' surfaces.

Figure 61. False-color lux scale from 0 to 3000 lux.

Through the metric of point-in-time illuminance, similar results demonstrated in previous chapter can be seen (Figure 62 to 64). With the dynamic shading screens, at 12 pm on each date the study area closed to the windows have illuminance less than 2,000 lux; at 9 am and 4 pm on each date, less study area receive illuminance over 3,000 lux which is deemed as having the potential for glare at that given point. At 4 pm on September 21st and December 21st, for example, it is clear to see that the dynamic shading screen is able to block the direct sunlight that causes issues of glare and overheat.

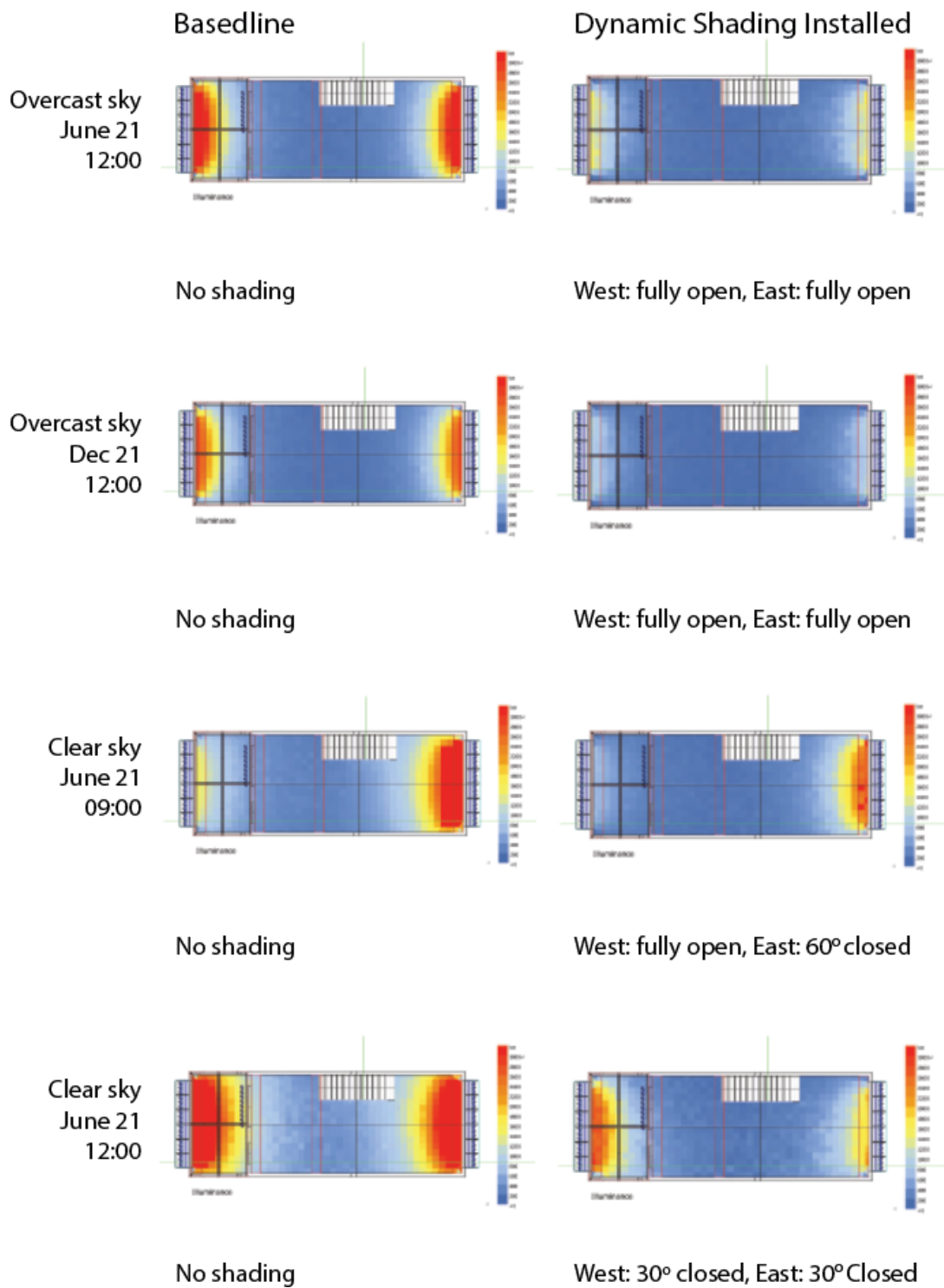


Figure 62. Point-in-time illuminance range A.

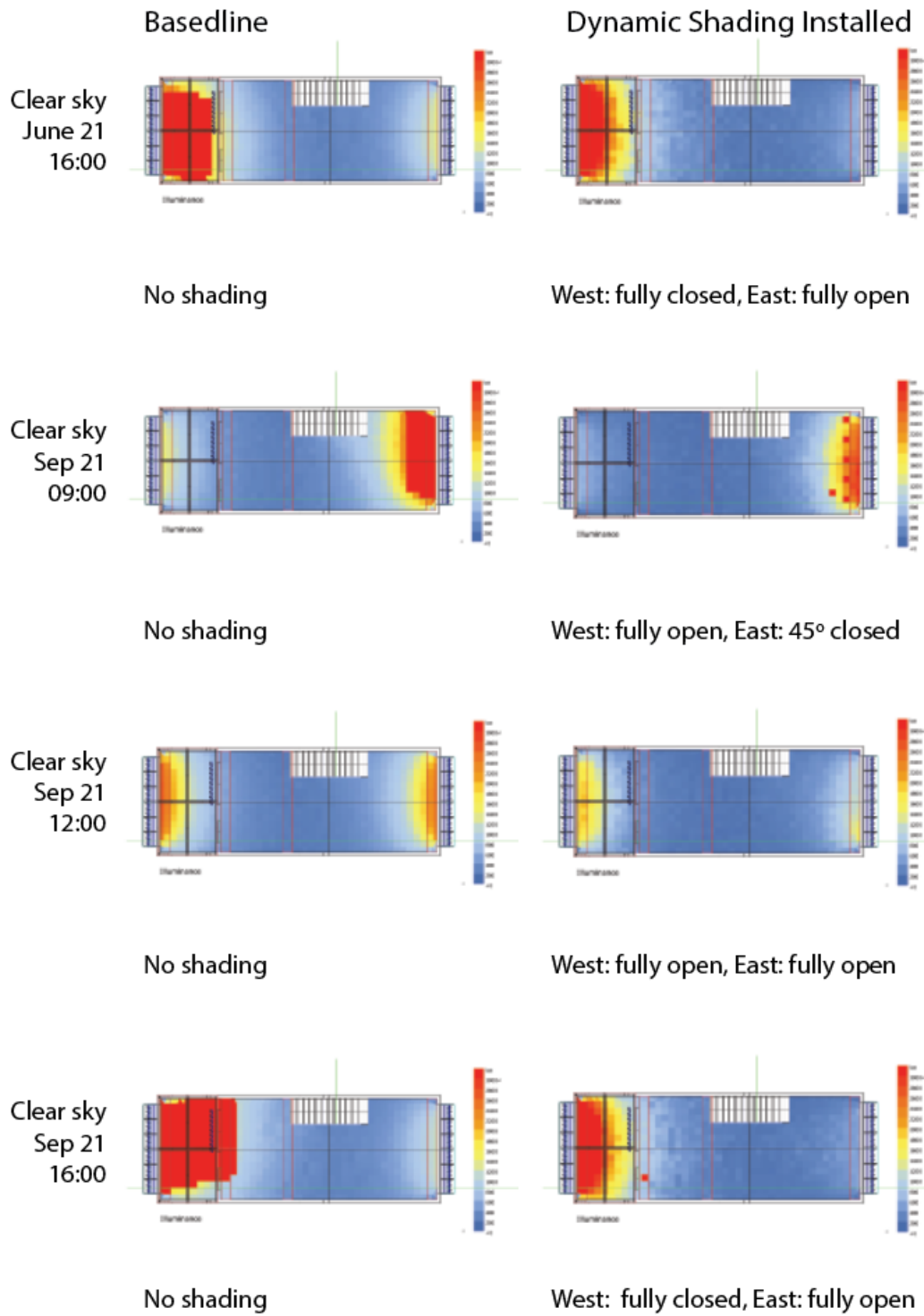


Figure 63. Point-in-time illuminance range B.

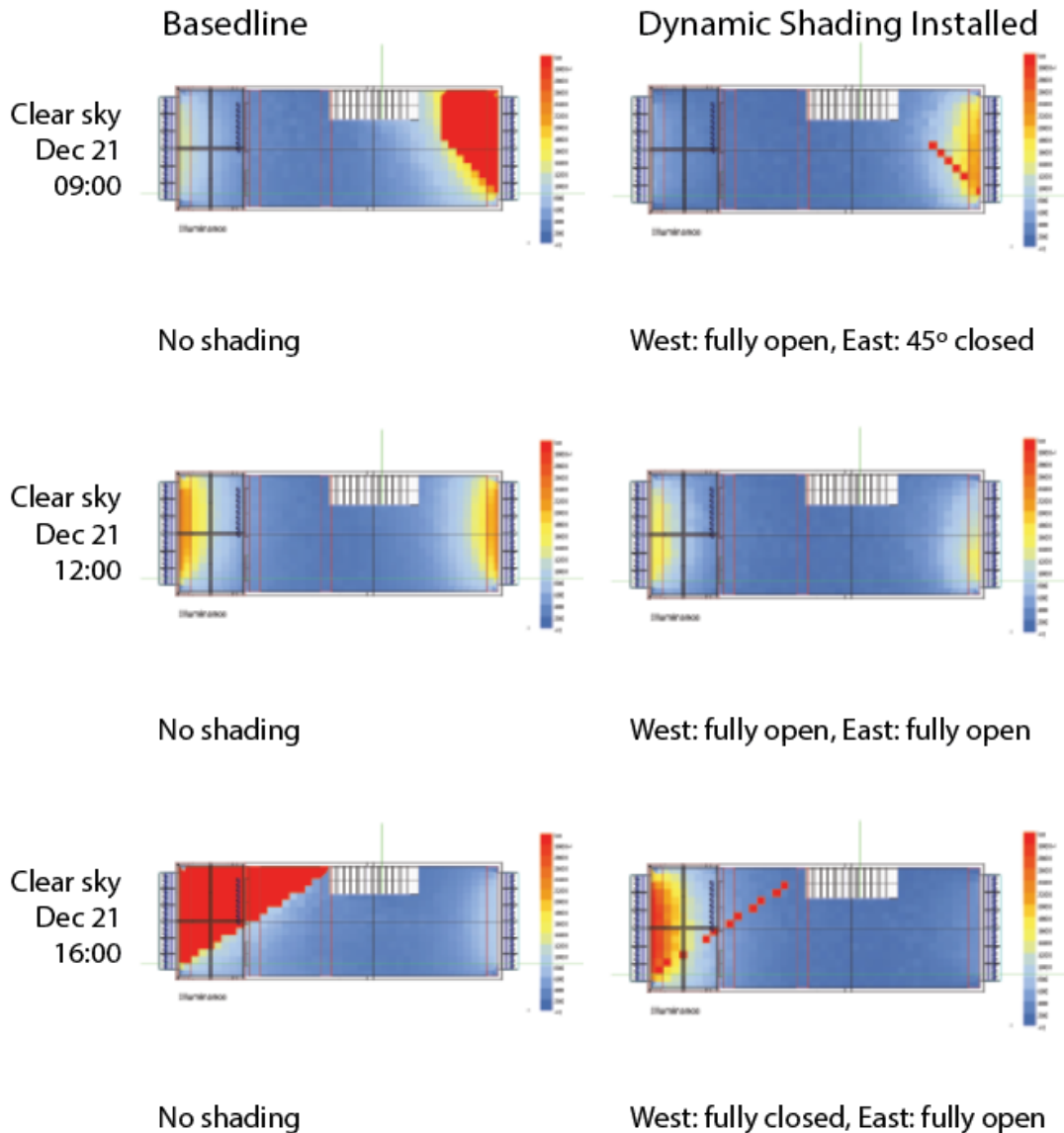


Figure 64. Point-in-time illuminance range C.

7.3 Annual Illuminance Testing

In this section, a grid-based annual illuminance analysis was conducted. Two measures were adopted to visualize the result: The first measure examines the percentage of hours that the indoor illuminance falls within the range of 100 to 3,000 lux (Figure 65 left) using the metric useful daylight autonomy (UDI) [31]. The second measure examines the percentage of hours that the indoor illuminance exceeds 3,000 lux (Figure 65 Right).

The scenario with no shading is set as the baseline. In the scenario with the dynamic shading screen, the rotatable fins are in their fully open state (all fins are perpendicular to the frame) when being simulated in Honeybee. Predictably, if the rotatable fins'

motion could be simulated in Honeybee, the annual illuminance level might be lower than the simulated setting. However, a worth noticing result still appears in the comparison between the baseline and the simulated scenario (Figure 66, 67).

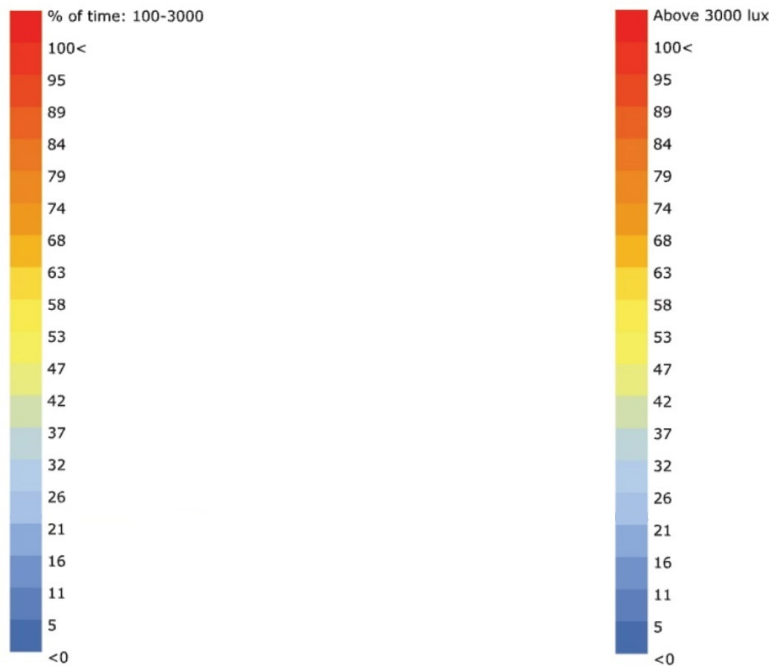


Figure 65. Annual illuminance received in the townhouse’s study area in percentage of hours in a year. Within 100 to 3,000 lux (Left); Above 3,000 lux (Right).

With the dynamic shading screen, the percentage of hours that the study area performs within the illuminance range from 100 to 3,000 (Figure 66) is significantly increased. With the dynamic shading screen’s intervention, there is a 40% increase in the time in range compared to the baseline (the blue area in Figure 66 left versus yellow and orange area Figure 66 right). Similarly, the area that is deeper in the space in the baseline (the orange area in Figure 66 left) improves by more than 5% growth as indicated by the area that turns from orange to red. The middle of the space falls outside of our range due to insufficient illuminance (Figure 66 Right). However, partitions are usually placed between the occupiable spaces (rooms) and the circulation (hallway), so the illuminance received in this area is not included in the evaluation. In Figure 67, it is clear to see that with the dynamic shading screen, the study area close to the windows has approximately 30% less hours in an over-lit condition (above 3,000 lux).

Baseline: no shading

With the dynamic shading screen

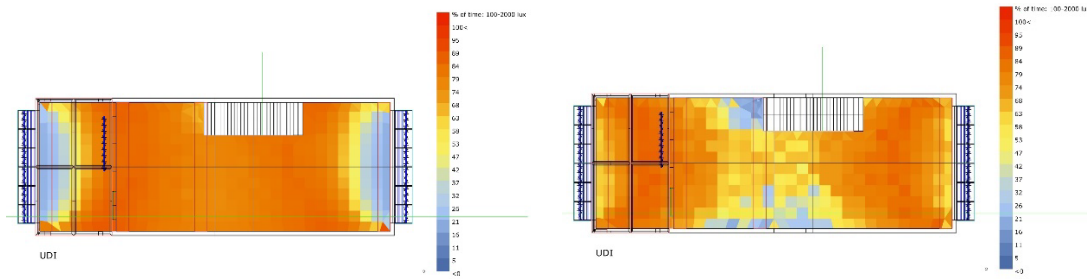


Figure 66. Annual illuminance within 100 to 3,000 lux in percentage of hours.

Baseline: no shading

With the dynamic shading screen

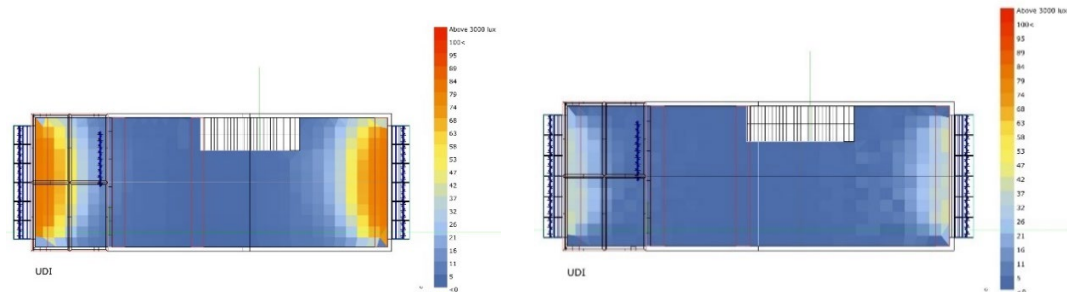


Figure 67. Annual illuminance above 3,000 lux in percentage of hours.

Chapter 8: Conclusion

8.1 Benefits for Residence's Occupants

For the residence's occupants, the benefits brought by the dynamic shading screen can be described from an external and an internal standpoint. From the external aspect, due to the rarity of dynamic shading device in Taiwan, the occupants can experience an innovative building appearance. The interaction between the weather and the dynamic shading screens makes building facades alive. With the dynamic shading screens, residential buildings will no longer have a static appearance, but have a protean characteristic that is changing along with the environment and users' behavior. For old buildings owners, the emergence of the dynamic shading screen provides an opportunity of façade renovation. The customizable options of the shading device provide the occupants great flexibility that could suit their demands to renovate their houses.

From the internal aspects, with the dynamic shading screens, the residence's occupants will be living in a space with better daylighting quality, thermal comfort, and with the sense of safety retained. Moreover, since the demand on cooling is

lowered by the dynamic shading screens, the occupants can pay less for electricity.

8.2 Benefits for Taiwan

As mentioned in Chapter 1, over 80% of the power generation in Taiwan relies on thermal power plants. 48% of these are coal-fired [32], which is one of the main sources of the air pollution in the country. According to the data published by *Taiwan Power Company*, coal-fired power plants exhaust **tons** of pollutants in a year including suspended particles, nitrogen oxides, and sulfur oxides, etc. In 2019, for example, the thermal power plants in Taiwan exhausted 14 (kg/MWh) suspended particles, 158 (kg/MWh) nitrogen oxides, and 125 (kg/MWh). The total energy generated by thermal power plants in 2019 was 140,578 GWh [33]. As a result, the pollutants exhausted by the thermal power plants not only impact the air quality in the local cities, they also impact the whole country when the air convection rate is low.

Based on the energy-saving performance results shown in Chapter 5, the dynamic shading screen is able to save 15% to 21% energy use per household depending on the housing typology. To illustrate how the dynamic shading screens mitigate the energy crisis and issue of air pollution, a comparison between power plants' capacity and the amount of energy saved by the dynamic shading screen is described below.

The numbers and power generation capacity of power plants in Taiwan are summarized in Table 10 [34]. Of the six coal-fired power plants, the ones in Taichung county and Linkou county are the two plants with the highest power generation capacity, 48,208 (GWh/yr) and 21,036 (GWh/yr) respectively. Furthermore, it is worth noticing that Taiwan, as a small country, the coal-fired power plant in Taichung county is the third largest one in the world [35].

Power Plants by fuel	Numbers	Capacity (MW)
Coal-fired	6	14,679
Natural Gas	12	17,809
Nuclear	2	3,872
Hydro	28	2,092
Wind	32	831
Solar	28	4,160

Table 10. Summary of power plants in Taiwan [34].

Based on the statistical data published by *Bureau of Energy*, residential buildings in Taiwan consume approximately 45,000 to 48,000 GWh per year [36]. Take 2019 as an

example, 47,189 GWh was consumed by residential buildings in the country.

To forecast the amount of energy saved by the dynamic shading screen we can calculate the reduced electricity consumption resulting from the implementation of dynamic shading screens in the residential building stock. Based on the high prevalence of the existing window grilles and the need for shading in Taiwan, the dynamic shading screens could be used on new build projects and might be a potential substitute for the existing window grilles if promoted by the government. If 50% of the residential buildings in Taiwan have the dynamic shading screen installed which save 20% energy use per household annually, after ten years the following calculation can be made:

$$\begin{aligned} &47,000 \text{ GWh/yr (electricity consumed by all residential buildings)} \\ &\quad \times 50\% \text{ (half of residential buildings that have dynamic shading screen)} \\ &\quad \times 20\% \text{ (energy saving per household)} \times 10 \text{ (years)} = 47,000 \text{ (GWh)} \end{aligned}$$

47,000 GWh could be saved after a ten-year implementation. 47,000 GWh is equivalent to the amount of energy generated by the thermal power plant in Taichung county or the amount of energy generated by two thermal power plants in Linkou county. As a result, the application of the dynamic shading screen is able to mitigate the entirety of the coal-fired power plants' emissions. Also, since less coal is burned for power generation, the Taiwanese government can reduce its reliance on imported coal.

In conclusion, the application of dynamic shading screen is able to bring numerous benefits to Taiwan from the domestic scale to the country's scale. Being situated in a tropical area means that the high demand for cooling is inevitable. However, there are many strategies for architects to deal with this challenging building context. The proposed dynamic shading screen or any kinds of high-performance shading device should be one of the solutions that help mitigate the stress. Architectural firms in Taiwan should regard the environmental challenges as one of the design drivers and conceive responding design languages that is suitable for the Taiwanese built environment. The Taiwanese government should also keep offering increased incentives to promote sustainable design. If these notions could be commonly acknowledged in Taiwan, the accumulation of each subtle change would be a great improvement.

Bibliography

- [1] "Climate." Cwb.gov.tw, www.cwb.gov.tw/V7e/climate/monthlyMean/tx.htm.
- [2] Liggett R, Miline M. *Climate Consultant 6.0*, *UCLA Energy Design Tools Group, Department of Architecture and Urban Design*, University of California, Los Angeles –software, 2016, retrieved from <http://energy-design-tools.aud.ucla.edu/climate-consultant/request-climate-consultant.php>.
- [3] "Climate." Cwb.gov.tw, www.cwb.gov.tw/V7e/climate/monthlyMean/tx.htm.
- [4] "Energy Statistics Annual Report." 經濟部能源局(Bureau of Energy, Ministry of Economic Affairs, R.O.C.) 全球資訊網, www.moeaboe.gov.tw/ECW/populace/content/SubMenu.aspx?menu_id=6977
- [5] "Statistic Chart." 經濟部能源局(Bureau of Energy, Ministry of Economic Affairs, Taiwan) 全球資訊網, www.boeaboe.gov.tw/ECW/populace/conetent/SubMenu.aspx?menu_id=867
- [6] "家庭節能應用技術手冊", 財團法人台灣綠色生產力基金會, Sept. 2017, www.ecct.org.tw/Knowledge/knowledge_more?id=d6a612a1155d48fab2f61ccb2f549a7b.
- [7] "Choose a Bulb: Null." *Philips Lighting*, 2020, www.usa.lighting.philips.com/consumer/choose-a-bulb.
- [8] "Refrigerators." *Panasonic*, 2020, www.panasonic.com/middleeast/en/consumer/home-appliances/refrigerators.html.
- [9] "Bosch Dishwashers 101." *Bosch*, 2020, <https://www.bosch-home.com/us/products/dishwashers>
- [10] "冷氣噸數換算" - 冷氣單位計算參考表, 台灣產業服務基金會, egov.ftis.org.tw/upload/2_%E5%86%B7%E6%B0%A3%E5%96%AE%E4%BD%8D%E8%A8%88%E7%AE%97%E5%8F%83%E8%80%83%E8%A1%A8.pdf.
- [11] *Convert Pyeong to Square Foot*, www.convertunits.com/from/pyong/to/square+foot.
- [12] "Ton of Refrigeration." *Wikipedia*, Wikimedia Foundation, 9 Nov. 2019, en.wikipedia.org/wiki/Ton_of_refrigeration.
- [13] 辛永勝, 楊朝景."鐵花窗." 老屋顏: 走訪全台老房子, 從老屋歷史、建築裝飾與時代故事, 尋訪台灣人的生活足跡, 馬可孛羅文化, 2015, pp. 18–23.
- [14] Hammad, et al. "The Energy Savings Potential of Using Dynamic External Louvers in an Office Building." *Energy & Buildings*, vol. 42, no. 10, 2010, pp. 1888–1895.
- [15] Favoino, et al. "Experimental Analysis of the Energy Performance of an ACTIVE, RESponsive and Solar (ACTRESS) Façade Module." *Solar Energy*, vol. 133, 2016,

pp.226–248.

- [16] Sjarifudin, et al. EPJ Web of Conferences, vol. 68,2014, pp. 00037–1-00037–7.
- [17] Ahmed, Mostafa M. S., et al. “Optimum Energy Consumption by Using Kinetic Shading System for Residential Buildings in Hot Arid Areas.” *International Journal of Smart Grid and Clean Energy*, 2016, pp. 121-128.
- [18] “Grasshopper 3D.” *Wikipedia*, Wikimedia Foundation, 22 May 2020, en.wikipedia.org/wiki/Grasshopper_3D.
- [19] “Rhinceros 3D.” *Wikipedia*, Wikimedia Foundation, 23 June 2020, en.wikipedia.org/wiki/Rhinceros_3D.
- [20] Murphy, Mark, et al. “Energy Savings Potential with Electrochromic Switchable Glazing.” *9th Nordic Symposium on Building Physics*, vol. 3, 2011, pp. 1281–1288.
- [21] Y. Elghazi, et al. “Daylighting driven design: optimizing kaleidocycle facade for hot arid climate.” *Aachen: Fifth German-Austrian IBPSA Conference*, RWTH Aachen University, 2014.
- [22] A. Fioravanti, et al. “ShoCK! - Sharing Computational Knowledge!”, *Proceedings of the 35th eCAADe Conference*, Volume 2, Sapienza University of Rome, Rome, Italy, 20-22 September 2017, pp. 231-240.
- [23] “DIVA.” *Solemnia LLC*, www.solemnia.com/Divia.html.
- [24] Mahmoud, and Elghazi. “Parametric-Based Designs for Kinetic Facades to Optimize Daylight Performance: Comparing Rotation and Translation Kinetic Motion for Hexagonal Facade Patterns.” *Solar Energy*, vol. 126, 2016, pp. 111–127.
- [25] L. Giovannini, et al. “Lighting and energy performance of an adaptive shading and daylighting system for arid climates.” *Energy Procedia*, vol. 78, 2015, pp. 370–375.
- [26] “Mashrabiya.” *Wikipedia*, Wikimedia Foundation, 27 June 2020, en.wikipedia.org/wiki/Mashrabiya.
- [27] Jacobson, M. Alexander. “Honeybee Wiki Home.” *GitHub*, 24 Feb. 2019, github.com/ladybug-tools/honeybee-legacy/wiki.
- [28] “住宅資訊 - 調查研究報告。” 肆、調查結果綜合分析-中華民國內政部營建署全球資訊網, 5 Dec. 2006, www.cpami.gov.tw/%E7%87%9F%E5%BB%BA%E7%BD%B2%E5%AE%B6%E6%97%8F/%E7%87%9F%E5%BB%BA%E6%A5%AD%E5%8B%99/%E4%BD%8F%E5%AE%85%E8%B3%87%E8%A8%8A/%E8%AA%BF%E6%9F%A5%E7%A0%94%E7%A9%B6%E5%A0%B1%E5%91%8A/7734-%E8%82%86%E3%80%81-%E8%AA%BF%E6%9F%A5%E7%B5%90%E6%9E%9C%E7%B6%9C%E5%90%88%E5%88%86%E6%9E%90.html.
- [29] “ASHRAE Climate Zone Map.” *ResearchGate*, American Society of Heating,

- Refrigerating and Air-Conditioning Engineers,
www.researchgate.net/figure/ASHRAE-climate-zone-map_fig6_323809391.
- [30] Lechner, Norbert. Heating, Cooling, Lighting: *Sustainable Design Methods for Architects*. Fourth ed., John Wiley & Sons, Inc., 2015, pp. 239.
- [31] Nabil, A, et al. Useful daylight illuminance: A new paradigm for assessing daylight in buildings. *Lighting Research & Technology – LIGHTING RES TECHNOL.* 37, 2005, pp. 41-59.
- [32] “火力發電結構.” 火力電廠環境保護, 台灣電力公司 (Taiwan Power Company), 2019, www.taipower.com.tw/tc/page.aspx?mid=216.
- [33] “空氣污染物排放源.” 火力電廠環境保護, 台灣電力公司 (Taiwan Power Company), 13 May 2020, www.taipower.com.tw/TC/page.aspx?mid=216&cid=167&cchk=52bd713e-a1f9-4acd-a29c-dcc554853239.
- [34] “各機組發電量.” 今日電力資訊, 台灣電力公司 (Taiwan Power Company), 2020, www.taipower.com.tw/tc/page.aspx?mid=206&cid=406&cchk=b6134cc6-838c-4bb9-b77a-0b0094afd49d.
- [35] “Taichung Power Plant.” Wikipedia, Wikimedia Foundation, 25 June 2020, en.wikipedia.org/wiki/Taichung_Power_Plant.
- [36] “住宅與服務業部門電力消費(歷年).” 能源統計月報, 經濟部能源局(Bureau of Energy, Ministry of Economic Affairs), 15 June 2020, www.moeaboe.gov.tw/ECW/populace/web_book/WebReports.aspx?book=M_CH&menu_id=142.